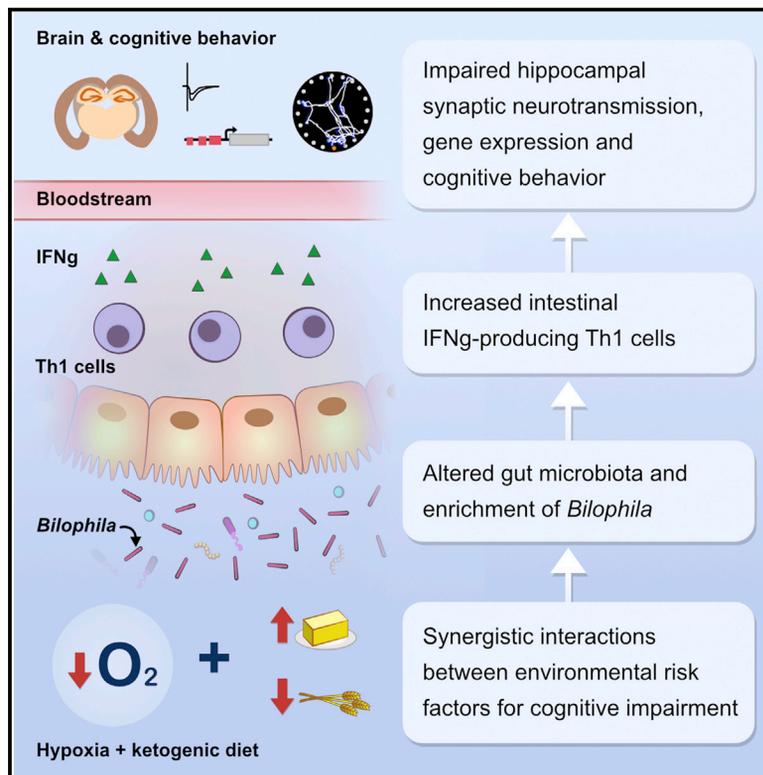# Alterations in the gut microbiota contribute to cognitive impairment induced by the ketogenic diet and hypoxia

Graphical abstract

Authors

Christine A. Olson, Alonso J. Iñiguez, Grace E. Yang, ..., Jacob T. Barlow, Rustem F. Ismagilov, Elaine Y. Hsiao

Correspondence

olsonca@g.ucla.edu (C.A.O.), ehsiao@g.ucla.edu (E.Y.H.)

In brief

Alterations in the gut microbiome are increasingly implicated in cognitive dysfunction. Olson et al. reveal that ketogenic diet and hypoxia synergistically impair cognitive behavior and modify the gut microbiota in mice. Select risk-associated bacteria are sufficient to disrupt hippocampal function and cognitive behavior via immune-mediated pathways.

Highlights

- The ketogenic diet and hypoxia synergistically impair cognitive behavior in mice

- Depleting or transplanting the gut microbiota modulates cognitive behavior in mice

- *Bilophila wadsworthia* disrupts cognitive behavior and hippocampal physiology

- IFNg-producing Th1 cells contribute to microbiota-mediated cognitive impairment

CellPress

Cell Host & Microbe

CellPress

Alterations in the gut microbiota contribute to cognitive impairment induced by the ketogenic diet and hypoxia

Christine A. Olson,[1,*] Alonso J. Iñiguez,[1] Grace E. Yang,[1] Ping Fang,[1] Geoffrey N. Pronovost,[1] Kelly G. Jameson,[1] Tomiko K. Rendon,[1] Jorge Paramo,[1] Jacob T. Barlow,[2] Rustem F. Ismagilov,[2] and Elaine Y. Hsiao[1,3,*]

[1]Department of Integrative Biology & Physiology, University of California, Los Angeles, Los Angeles, CA 90095, USA
[2]Division of Chemistry & Chemical Engineering, California Institute of Technology, Pasadena, CA 91108, USA
[3]Lead contact
*Correspondence: olsonca@g.ucla.edu (C.A.O.), ehsiao@g.ucla.edu (E.Y.H.)
https://doi.org/10.1016/j.chom.2021.07.004

SUMMARY

Many genetic and environmental factors increase susceptibility to cognitive impairment (CI), and the gut microbiome is increasingly implicated. However, the identity of gut microbes associated with CI risk, their effects on CI, and their mechanisms remain unclear. Here, we show that a carbohydrate-restricted (ketogenic) diet potentiates CI induced by intermittent hypoxia in mice and alters the gut microbiota. Depleting the microbiome reduces CI, whereas transplantation of the risk-associated microbiome or monocolonization with *Bilophila wadsworthia* confers CI in mice fed a standard diet. *B. wadsworthia* and the risk-associated microbiome disrupt hippocampal synaptic plasticity, neurogenesis, and gene expression. The CI is associated with microbiome-dependent increases in intestinal interferon-gamma (IFNg)-producing Th1 cells. Inhibiting Th1 cell development abrogates the adverse effects of both *B. wadsworthia* and environmental risk factors on CI. Together, these findings identify select gut bacteria that contribute to environmental risk for CI in mice by promoting inflammation and hippocampal dysfunction.

INTRODUCTION

Cognitive impairment (**CI**) is characterized by deficient attention, causal reasoning, and learning and memory, and afflicts a reported 3%–19% of people over 65 years old worldwide (Mavrodaris et al., 2013). In addition to its prevalence in aging and aging-related neurodegenerative disorders such as Alzheimer's and Parkinson's disease, CI is also associated with a wide variety of chronic metabolic, immunological, neuropsychiatric, and sleep disorders, making CI a pressing global health concern. Genetic, environmental, and behavioral factors together predispose to CI, and many biological pathways are implicated, including neuroinflammation, mitochondrial dysfunction, and blood-brain barrier disruptions (Han et al., 2020; Sweeney et al., 2018). In particular, both hypoxia-associated physiological stressors, such as high altitude, strenuous activity, sleep apnea, vascular dysfunction (Akinyemi et al., 2013; Das et al., 2018; Duncombe et al., 2017; Pun et al., 2019; Solis et al., 2020; Zhao, and Gong, 2015), and the high-fat high-sugar "Western" diet (Kanoski and Davidson, 2011; Noble et al., 2017; Pistell et al., 2010; Wei et al., 2018) are well-known to increase risk for CI, whereas the high-fat low-carbohydrate ketogenic diet is being explored for treatment of CI, with variable results to date (Bahr et al., 2020; Lauritzen et al., 2016; Nagpal et al., 2019; Ota et al., 2019; Phillips

et al., 2018; van Berkel et al., 2018; Zhao et al., 2004). Despite many studies on environmental risks for CI, exactly how environmental factors, such as diet and physical stress, modify susceptibility for CI remains poorly understood.

The gut microbiome is emerging as an important mediator of environmental contributions to host health and disease. Environmental factors, including diet, stress, and age can shape the composition and function of the gut microbiota (Marques et al., 2010; O'Toole and Jeffery, 2015; Rea et al., 2016). Alterations in the gut microbiome can, in turn, mediate effects of environmental challenges on various behavioral abnormalities, including impaired communication in response to maternal immune activation, anxiety-related behavior in response to stress, and reduced sociability in response to high-fat diet (Bravo et al., 2011; Buffington et al., 2016; Gareau et al., 2011; Hsiao et al., 2013; Savignac et al., 2015). Moreover, depleting the microbiome by germ-free rearing or antibiotic treatment disrupts cognitive performance across various tasks for working and spatial memory when compared with controls raised with conventional microbiomes (Chu et al., 2019; D'Amato et al., 2020; Fröhlich et al., 2016; Gareau et al., 2011; Hoban et al., 2016; Sampson and Mazmanian, 2015; Vuong et al., 2017; Yu et al., 2019). These animal studies provide fundamental proof-of-concept that investigating interactions between the gut microbiome and environmental risk factors for CI may reveal

previously uncharacterized cellular and molecular signaling pathways that regulate CI.

Herein, we examine the effects of two environmental modifiers of CI—intermittent hypoxia and the ketogenic diet —on the gut microbiota, neurophysiology, and cognitive behavior. We evaluate causal roles for environmentally induced changes in the gut microbiome in promoting CI, and further identify specific microbial taxa that contribute to environmental risk for impaired hippocampal function and cognitive deficits. Finally, we investigate functional effects of risk-associated microbes to reveal that microbial stimulation of type-1 immune responses contribute to microbiome-mediated environmental susceptibility to CI.

RESULTS

The ketogenic diet exacerbates hypoxia-induced cognitive impairment

Hypoxia is an environmental risk factor for CI associated with high altitude exposure, sleep apnea, vascular dementia, and Alzheimer's disease, among many other pathological conditions (Biswal et al., 2016; de Aquino Lemos et al., 2012; Desbonnet et al., 2014; Giuliani et al., 2019; Qaid et al., 2017). To determine the impact of acute intermittent hypoxia on cognitive behavior, conventional mice (specific pathogen-free, **SPF**) consuming a control diet (**CD,** Table S1) were subjected to 6 h of restricted 12% oxygen (normobaric hypoxia, **Hyp**) or ambient 21% oxygen (normoxia, **Mock**) daily for 5 days, a regimen within the range of hypoxic treatments sufficient to induce CI in mice (Deguil et al., 2016). Following a 4-day recovery period, mice were then evaluated for cognitive and spatial learning and memory behavior in the Barnes maze task (Figure 1A). Consistent with prior literature (Aubrecht et al., 2015; Mei et al., 2020), mice exposed to Hyp exhibited impaired cognitive behavior in the Barnes maze, as indicated by increased latency to enter the escape box, errors made, and use of random search strategy as compared with Mock controls (Figures 1B–1F). These impairments were observed even on the first trial of testing, suggesting that CI that can include disrupted learning and memory, in addition to deficits in other underlying cognitive processes (Li et al., 2013; Shen et al., 2020). There were no significant differences in velocity or total distance traveled in the Barnes maze (Figures S1A and S1F), suggesting no confounding abnormalities in motor function. There were also no differences in performance in the open field test and prepulse inhibition task, suggesting no overt alterations in stress-induced exploration or sensorimotor gating (Figure S1N). These results indicate that acute intermittent hypoxia impairs cognitive behavior in mice, which is consistent with previous reports (Aubrecht et al., 2015; Mei et al., 2020).

High dietary fat intake modifies cognitive behavior in humans and animal models. For example, consumption of the high-fat high-sugar "Western" diet leads to deficits in memory speed, flexibility, prospective memory, and spatial learning and memory (Beilharz et al., 2015; Cordner and Tamashiro, 2015; Kanoski and Davidson, 2011; Noble et al., 2017; Pistell et al., 2010; Wei et al., 2018), particularly in response to physical or psychosocial stress (Arcego et al., 2018; Kesby et al., 2015). In contrast, the ketogenic diet (KD), which is also based on high fat intake, but includes carbohydrate restriction, is used clinically for its neuroprotective effects in refractory epilepsy, and is now increasingly

applied to human neurodegenerative and cognitive disorders, despite limited experimental studies in this context (McDonald and Cervenka, 2019; Vinciguerra et al., 2020). Although some studies suggest that the KD may protect against CI, other studies report that it may be detrimental (Lauritzen et al., 2016; Zhao et al., 2004). To examine effects of the KD on cognitive behavior, SPF mice were pretreated with the ketogenic chow, used commonly to model the classical clinical KD (Dutton et al., 2011; Samala et al., 2008), and subjected to Mock or Hyp as described earlier (Figure 1G). Mice fed the KD exhibited no significant differences in cognitive behavior in the Barnes maze, as compared with mice fed the vitamin and mineral-matched CD (Figure 1, **SPF CD Mock** versus **SPF KD Mock**), indicating that the KD alone has no overt effect on cognitive behavior in the Barnes maze. Notably, however, mice fed the KD and exposed to Hyp (**SPF KD Hyp**) exhibited a substantial increase in latency to enter the escape box, errors made, and random search strategy as compared with Mock controls fed the KD (**SPF KD Mock**) (Figures 1H–1L). The Hyp-induced behavioral impairment was significantly more severe in KD-fed mice than in CD-fed mice (Figures 1 and S1K–S1M). There was no significant difference across experimental groups in velocity or total distance traveled in the Barnes maze (Figures S1B and S1G) or in performance in the open field and prepulse inhibition tasks (Figures S1N–S1R). These results indicate that the KD potentiates the adverse effects of Hyp on cognitive behavior in mice, and further highlight synergistic interactions between diet and hypoxic stress as environmental risk factors for CI.

Ketogenic diet- and hypoxia-associated alterations in the gut microbiota impair cognitive behavior

Environmental factors, including diet and stress, play important roles in shaping the composition and function of the gut microbiota (David et al., 2014; Lobionda et al., 2019; Sbihi et al., 2019; Tripathi et al., 2018; van de Wouw et al., 2018). To gain insight into whether the gut microbiota contributes to KD- and Hyp-induced disruptions in cognitive behavior, SPF mice were pretreated with broad-spectrum antibiotics (**Abx**) to deplete the gut microbiota prior to KD and Hyp exposure (Figure 2A) (Reikvam et al., 2011). Compared with vehicle-treated controls, KD- and Hyp-exposed mice that were pretreated with Abx exhibited improved cognitive performance, as indicated by decreased latency to enter the escape box, errors made, and use of random search strategy (Figures 2B–2F, **SPF KD Hyp** versus **Abx KD Hyp**). Results for each of these behavioral parameters were comparable with those seen in Mock controls fed the KD (Figures 2B–2F, S1C, and S1H; **Abx KD Hyp** versus **SPF KD Mock**), suggesting that depletion of the microbiota abrogated KD and Hyp-induced impairments in cognitive behavior. To determine whether mice reared in the absence of the microbiome exhibit similar protection against KD- and Hyp-induced CI, germ-free (GF) mice were fed the KD and exposed to Hyp under sterile conditions and then tested in the Barnes maze using aseptic technique. qPCR for fecal loads of the 16S rRNA gene after the last day of Barnes maze testing revealed that the behaviorally tested GF mice exhibit 16S rRNA gene levels comparable with those seen in untested GF mice, suggesting no overt contamination during behavioral testing (Figure S2I). However, given the possibility that there could be
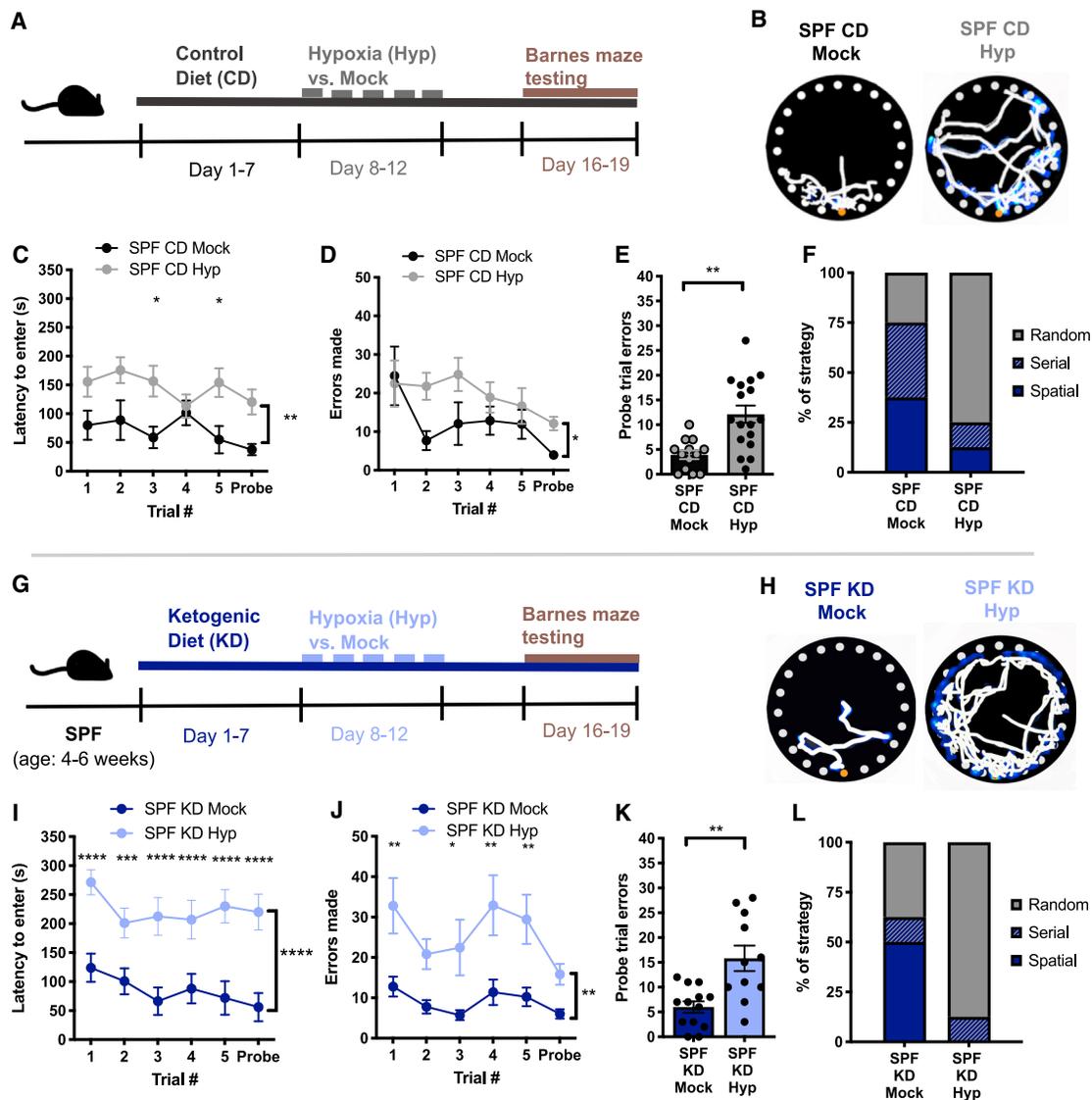
Cell Host & Microbe
Article

Figure 1. The ketogenic diet potentiates hypoxia-induced impairments in cognitive behavior
(A and B) (A) Experimental timeline (B) Representative Barnes maze traces for SPF mice fed the CD and exposed to Mock or Hyp. White lines indicate movement trajectories, whereas blue hues denote increasing durations of time spent at a specific location. Orange circles indicate the escape hole.
(C) Latency to enter the escape hole of the Barnes maze across six 300-s trials (two-way ANOVA with Sidak, n = 13–17).
(D) Errors made as measured by number of incorrect nose pokes (two-way ANOVA with Sidak, n = 13–17).
(E) Errors made during the final trial (probe) (unpaired two-tailed Students t test, n = 13–17).
(F) Search strategy used during the probe trial (n = 13–17).
(G) Experimental timeline (n = 11–13).
(H) Representative Barnes maze traces for SPF mice fed the KD and exposed to Mock or Hyp.
(I) Latency to enter the escape hole across six 300-s trials (two-way ANOVA with Sidak, n = 11–13).
(J) Errors made (two-way ANOVA with Sidak, n = 11–13).
(K) Errors made during the probe trial (unpaired two-tailed Students t test, n = 11–13).
(L) Search strategy used during the probe trial. (n = 11–13). Data are presented as mean ± SEM. * p < 0.05, **p < 0.01, ***p < 0.001, ****p < 0.0001. n.s., not statistically significant; SPF, specific pathogen-free (conventionally colonized); CD, control diet; KD, ketogenic diet; Mock, intermittent normoxia exposure; Hyp, intermittent hypoxia exposure.

low-level contamination within typical variation seen in fecal 16S rRNA gene levels from GF mice, we refer to behaviorally tested GF mice as "**ex-GF**." Consistent with results from Abx treatment, ex-GF mice fed the KD were resistant to Hyp-induced CI in the Barnes maze (Figures S2A–S2H). Compared with KD-fed

SPF mice, however, ex-GF mice fed the KD exhibited impaired cognitive behavior at baseline, as indicated by increased latency to enter and increased errors made in the Barnes maze. This suggests detrimental effects of KD particularly in mice raised GF (Gareau et al., 2011). To additionally evaluate potential
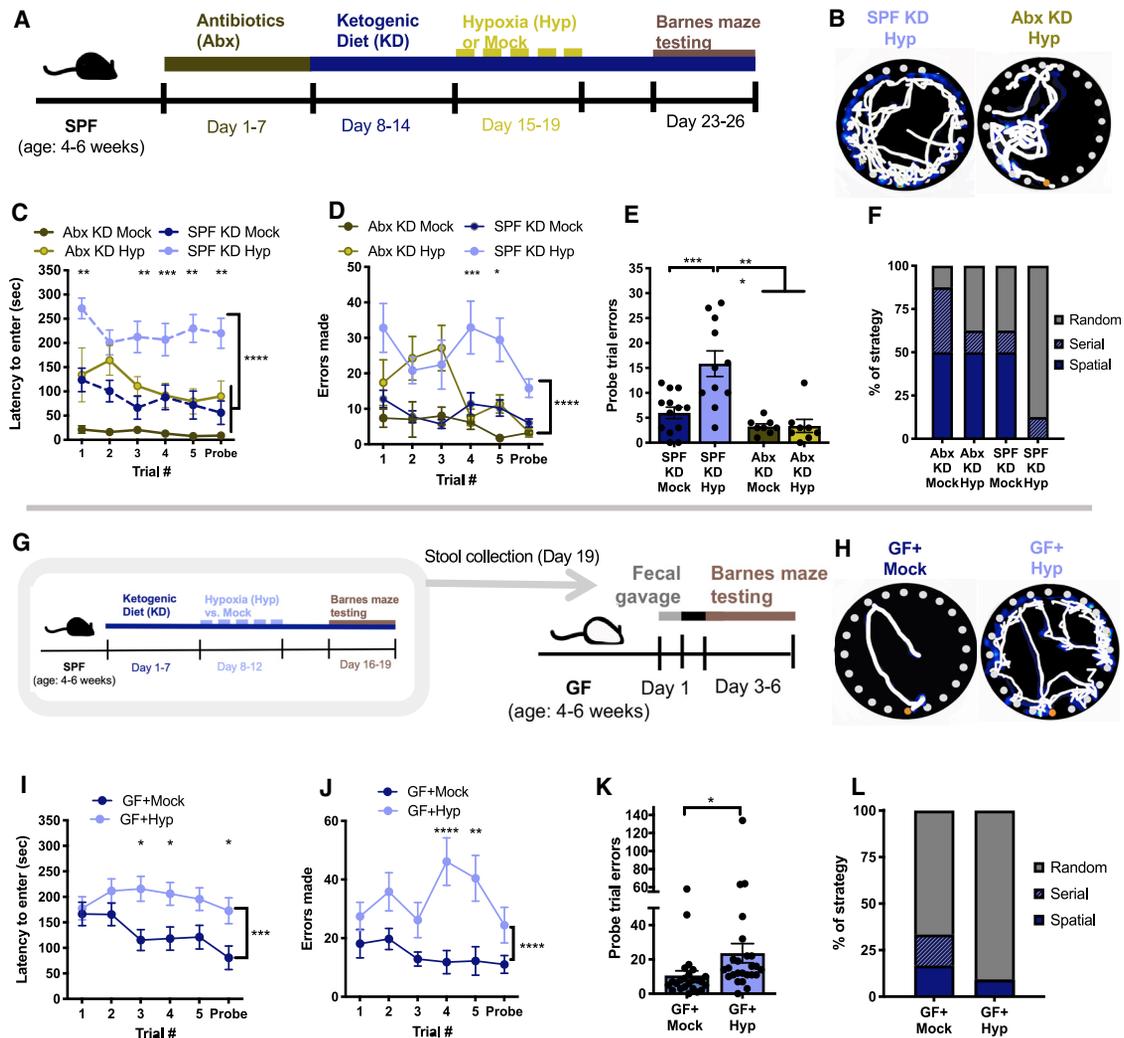
Figure 2. Alterations in the gut microbiota contribute to ketogenic diet and hypoxia-induced impairments in cognitive behavior

(A) Experimental timeline.

(B) Representative Barnes maze traces for SPF or Abx mice fed the KD and exposed to Hyp. White lines indicate movement trajectories, whereas blue hues denote increasing durations of time spent at a particular location. Orange circles indicate the escape hole.

(C) Latency to enter the escape hole of the Barnes maze across six 300-s trials (two-way ANOVA with Sidak, n = 8 for Abx groups; SPF data are as in Figure 1).

(D) Errors made as measured by number of incorrect nose pokes (two-way ANOVA with Sidak, n = 8 for Abx groups; SPF data are as in Figure 1).

(E) Errors made during the probe trial (one-way ANOVA with Dunnett, n = 8 for Abx groups; SPF data are as in Figure 1).

(F) Search strategy used during probe trial (n = 8).

(G) Experimental timeline.

(H) Representative Barnes maze traces for GF transplanted with fecal microbiota from SPF KD Mock or SPF KD Hyp donors. Transplanted recipient mice receiving SPF KD Mock microbiota are denoted GF+Mock. Transplanted recipient mice receiving SPF KD Hyp microbiota are denoted GF+Hyp.

(I) Latency to enter the escape hole (two-way ANOVA with Sidak, n = 23).

(J) Errors made (two-way ANOVA with Sidak, n = 23).

(K) Errors made during the probe trial (unpaired two-tailed Students t test, n = 23).

(L) Search strategy used during probe trial. (n = 14–15). Data are presented as mean ± SEM * p < 0.05, **p < 0.01, ***p < 0.001, ****p < 0.0001. n.s., not statistically significant; SPF, specific pathogen-free (conventionally colonized); Abx, treated with antibiotics (ampicillin, vancomycin, metronidazole, and neomycin); KD, ketogenic diet; Mock, intermittent normoxia exposure; Hyp, intermittent hypoxia exposure; GF, germ-free; GF+Mock, GF mice transplanted with microbiota from SPF mice fed KD and exposed to Mock; GF+Hyp, GF mice transplanted with microbiota from SPF mice fed KD and exposed to Hyp.

off-target effects of antibiotic treatment, GF mice were pretreated with Abx to determine whether antibiotics can impact hypoxia-induced impairments in Barnes maze behavior in the absence of the microbiome. Abx treatment had no significant effect on latency to enter in the Barnes and significantly increased

errors made by KD-fed ex-GF mice, regardless of Mock or Hyp treatment (Figures S2J–S2O). This indicates that Abx pretreatment has microbiome-independent effects that increase errors made by ex-GF mice in the Barnes maze and further suggests that microbiome-dependent effects drive the Abx-induced
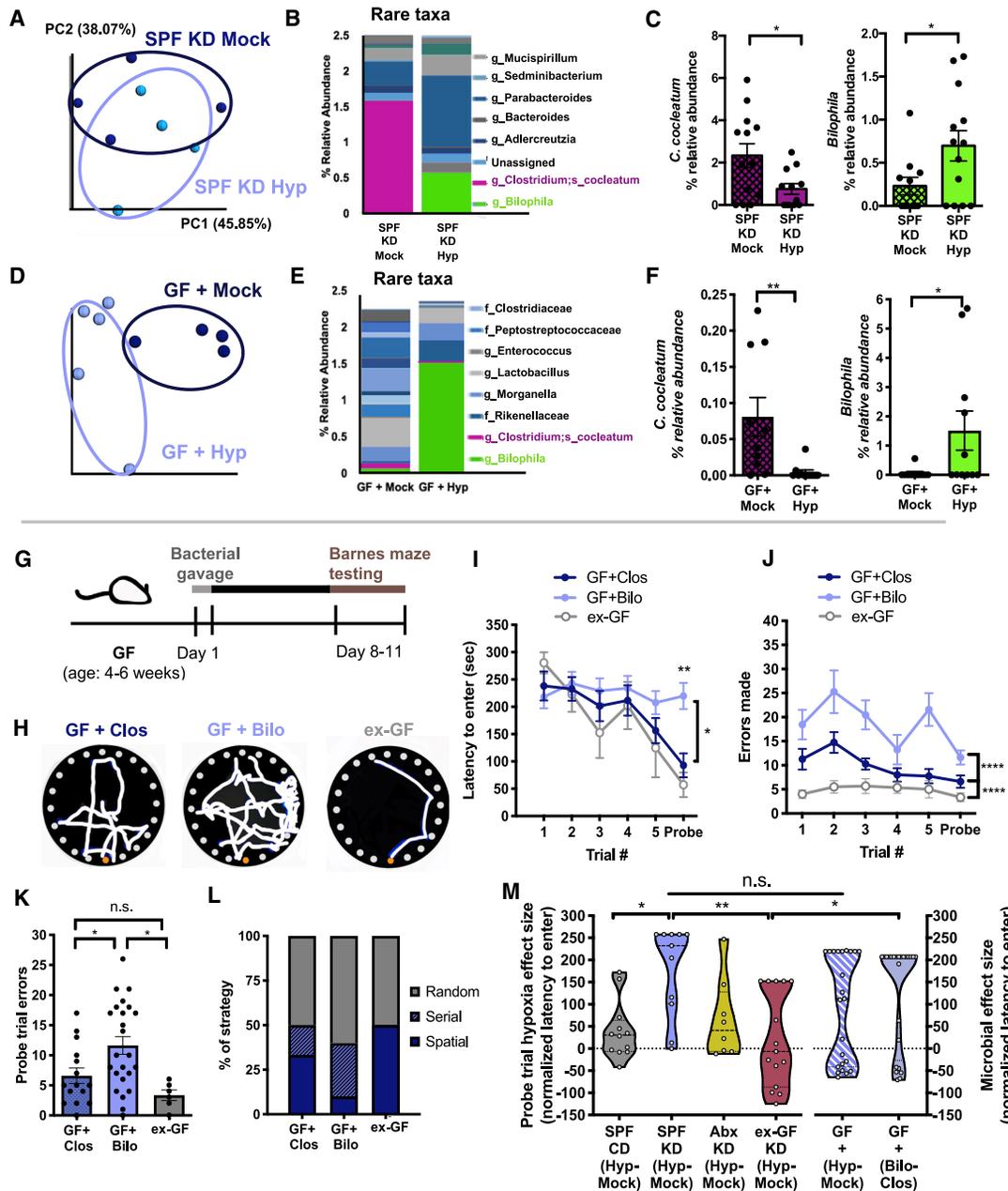
Figure 3. *Bilophila* is enriched by the ketogenic diet and hypoxia, and sufficiently impairs cognitive behavior

(A) Principal coordinates analysis of weighted UniFrac distance based on 16S rRNA gene profiling of feces from SPF mice fed KD and exposed to Hyp or Mock (n = 4 cages).

(B) Average taxonomic distributions of low abundance bacteria (n = 13 cages).

(C) Relative abundances of *Clostridium cocleatum* (left) and *Bilophila* spp. (right) in fecal microbiota (Kruskal-Wallis with Bonferroni, n = 13 cages).

(D) Principal coordinates analysis of weighted UniFrac distance based on 16S rRNA gene profiling of feces from GF mice transplanted with fecal microbiota from SPF KD Mock or SPF KD Hyp mice (in A–C) (n = 4–5 cages).

(E) Average taxonomic distributions of low abundance bacteria (n = 9 cages).

(F) Relative abundances of *C. cocleatum* (left) and *Bilophila* spp. (right) in fecal microbiota (Kruskal-Wallis with Bonferroni, n = 9 cages).

(G) Experimental timeline.

(H) Representative Barnes maze traces for GF mice monocolonized with Clos or Bilo. White lines indicate movement trajectories, whereas blue hues denote increasing durations of time spent at a particular location. Orange circles denote the escape hole.

(I) Latency to enter the escape hole across six 300-s trials for ex-GF mice and GF mice monocolonized with Clos or Bilo (two-way ANOVA with Sidak, n = 15, 24, 6).

(J) Errors made (two-way ANOVA with Sidak, n = 15, 24, 6).

(K) Errors made during the probe trial (unpaired two-tailed Students t test, n = 15, 24, 6).

(L) Search strategy used during probe trial (n = 15, 24, 6).

(legend continued on next page)

reductions in errors made by SPF KD Hyp mice in the Barnes maze (Figures 2D and 2E). Altogether, these data suggest that depletion of the gut microbiota prevents the synergistic effects of KD and Hyp on CI in mice.

To further test whether microbiota alterations in response to KD and Hyp contribute to disruptions in cognitive behavior, GF mice were transplanted with fecal microbiota from donor SPF mice fed KD and exposed to either Hyp or Mock (**GF + Hyp** and **GF + Mock**, respectively) (Figure 2G). Compared with controls colonized with the KD and Mock-associated microbiota, mice colonized with KD and Hyp-associated microbiota exhibited poor cognitive performance (Figures 2H–2L, S1D, and S1I), akin to that seen in mice fed KD and exposed to Hyp (Figures 1H–1L). Relative to SPF mice, transplanted control mice exhibited impaired performance on the first trial that improved with subsequent trials of the task, which may reflect initial confounding effects of GF status on behavior. Taken together, these results indicate that (1) the KD potentiates Hyp-induced impairments in cognitive behavior (Figures 1 and S1K–M), (2) depletion of the microbiota prevents the adverse synergistic effects of KD and Hyp on cognitive behavior (Figures 2A–2F), and (3) transplantation of the KD- and Hyp-associated microbiota into naive GF mice impairs cognitive behavior (Figures 2G–2L). These results strongly suggest that changes in the gut microbiota contribute to KD- and Hyp-induced impairments in cognitive behavior in mice.

Bilophila is enriched by the ketogenic diet and hypoxia and impairs cognitive behavior

To identify candidate microbial taxa that may be responsible for promoting KD- and Hyp-induced abnormalities in cognitive behavior, fecal microbiota were sequenced from SPF mice fed KD and exposed to Hyp or Mock (Figures 1G–1L), as well as from the mice transplanted with the corresponding microbiota from those SPF mice (Figures 2G–2L). Although there were no global alterations in the microbiota of mice fed KD and exposed to Hyp (Figures 3A and S3), select bacterial taxa were significantly altered in the Hyp group, compared with Mock controls (Figures 3B and 3C; Table S2). In particular, the relative abundances of *Clostridium cocleatum* were reduced in Hyp-exposed animals fed KD, whereas *Bilophila* species were elevated in Hyp-exposed animals fed KD (Figures 3B and 3C). The absolute abundance of *Bilophila* species was enriched particularly in mice exposed to both KD and Hyp, but not in mice exposed to either KD or Hyp alone (Figure S3E). This aligns with the observed synergistic effects of KD and Hyp on CI (Figures 1 and S1K–S1M), and with previous reports that dietary fat favors the growth of *Bilophila*, an obligate anaerobic pathobiont, in mice (Devkota et al., 2012). Similar reductions in *C. cocleatum* and increases in *Bilophila* were seen in mice transplanted with KD and Hyp-associated microbiota (Figures 3D–3F; Table S2). Overall,

these results reveal that KD and Hyp together enrich *Bilophila* and also impair cognitive behavior in mice.

To test whether *Bilophila* may contribute to the CI induced by KD and Hyp exposure, GF mice fed standard chow were monocolonized with *Bilophila wadsworthia* and tested for cognitive behavior, relative to GF mice and GF mice monocolonized with *C. cocleatum* (Figure 3G). *B. wadsworthia* was selected because it exhibited the highest sequence identity to the *Bilophila* operational taxonomic units elevated in mice fed KD and exposed to Hyp (Figures 3B and 3C). Mice colonized with *B. wadsworthia* exhibited impaired cognitive behavior compared with ex-GF and *C. cocleatum*-colonized controls, with no overt deficits in motor ability (Figures 3H–3L, S1E, and S1J). Notably, there were no statistically significant differences between ex-GF and *C. cocleatum*-colonized mice in latency to enter the escape box or errors made during the probe trial of the Barnes maze test, suggesting detrimental effects of *B. wadsworthia*, rather than beneficial effects of *C. cocleatum*, on cognitive behavior (Figures 3H–3L, S1E, and S1J). The effect of *B. wadsworthia* on CI during the probe trial of the Barnes maze assay was comparable with that seen with exposure to KD and Hyp and with transplantation of the KD- and Hyp-associated microbiota (Figure 3M). Overall, these data reveal that monocolonization with *B. wadsworthia* phenocopies the adverse effects of the KD- and Hyp-associated microbiota on cognitive behavior in mice.

The gut microbiota, and *Bilophila* in particular, modulates hippocampal activity

The hippocampus is sensitive to alterations in diet and hypoxic stress and is a critical site for learning and memory (Goldbart et al., 2006; Gozal et al., 2002; Kanoski and Davidson, 2011; Kanoski et al., 2010; Titus et al., 2007). To study effects of the KD and Hyp, and potential roles for the microbiota, on hippocampal physiology, field potential recordings were acquired from acute hippocampal slices from SPF mice fed KD and exposed to Hyp or Mock, as well as from GF mice colonized with *B. wadsworthia* or *C. cocleatum*. Compared with Mock-exposed controls, KD-fed mice that were exposed to Hyp exhibited significant reductions in hippocampal long-term potentiation (**LTP**, Figures 4A and 4B), population spike relative to field excitatory postsynaptic potential (**fEPSP**) slope, as a measure of excitatory postsynaptic potential spike coupling (Figure 4C) and paired-pulse facilitation (Figure 4D). Pretreatment with Abx diminished these abnormalities in hippocampal synaptic physiology (Figures S4A-S4D), suggesting that the gut microbiome contributes to the adverse effects of KD and Hyp on hippocampal physiology. Consistent with this, mice monocolonized with *B. wadsworthia* exhibited reduced hippocampal LTP (Figures 4E and 4F), reduced fiber volley amplitude versus fEPSP slope (Figure 4G) and reduced paired-pulse facilitation (Figure 4H) when compared with *C. cocleatum*-colonized controls. The

(M) Effect size of hypoxia on latency to enter the escape hole during the probe trial, as measured by the difference between Hyp groups and respective Mock controls for SPF, Abx, ex-GF, microbiota-transplanted (GF+Hyp-Mock), or monocolonized (GF+Bilo-Clos) mice fed CD or KD (two-way ANOVA with Dunnett, n = 8–24). Data are presented as mean ± SEM * p < 0.05, **p < 0.01, ***p < 0.001. n.s., not statistically significant; SPF, specific pathogen-free (conventionally colonized); KD, ketogenic diet; Mock, intermittent normoxia exposure; Hyp, intermittent hypoxia exposure; GF, germ-free; GF+Mock, GF mice transplanted with SPF KD Mock microbiota; GF+Hyp, GF mice transplanted with SPF KD Hyp microbiota; GF+Clos, GF mice monocolonized with *C. cocleatum*; GF+Bilo, GF mice monocolonized with *B. wadsworthia*; Abx, treated with antibiotics (ampicillin, vancomycin, metronidazole, and neomycin); CD, control diet; ex-GF, behaviorally tested GF mice.
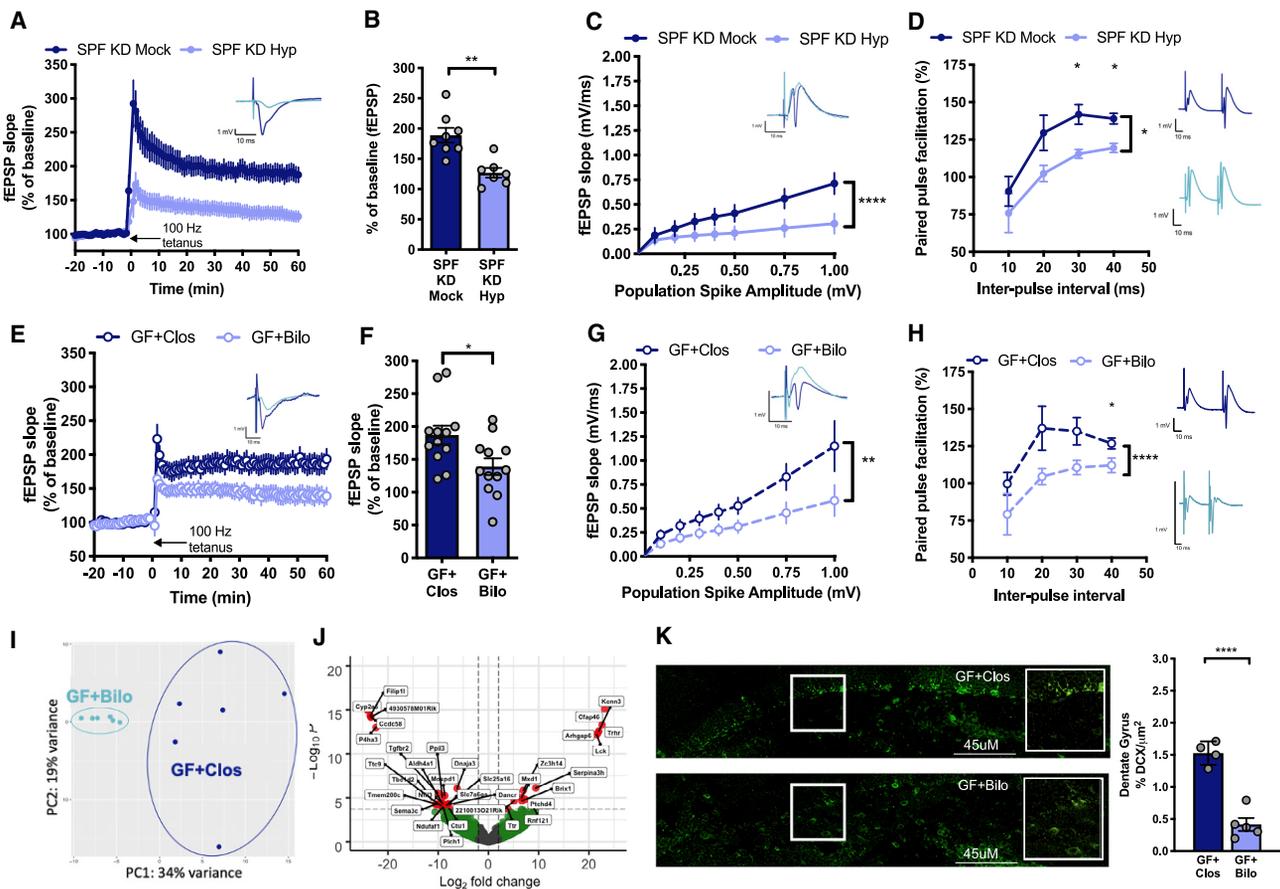
Figure 4. *Bilophila* colonization phenocopies ketogenic diet and hypoxia-induced impairments in hippocampal activity

(A) Hippocampal long-term potentiation (LTP) as indicated by fEPSP slope in response to 100 Hz tetanus, expressed as a percentage of 20-min baseline signal, from slice electrophysiology of brains from SPF mice fed KD and exposed to Hyp or Mock (n = 7–8).

(B) Average fEPSP slope during the last 5 min of hippocampal LTP recording (unpaired two-tailed Students t test, n = 7–8).

(C) Hippocampal population spike amplitude versus fEPSP slope (two-way ANOVA with Sidak, n = 7–8).

(D) Hippocampal paired pulse facilitation (two-way ANOVA with Sidak, n = 7–8).

(E) Hippocampal LTP from GF mice monocolonized with Clos or Bilo (n = 12).

(F) Average fEPSP slope during the last 5 min of hippocampal LTP recording (unpaired two-tailed Students t test, n = 12).

(G) Hippocampal population spike amplitude versus fEPSP slope (two-way ANOVA with Sidak, n = 6-10).

(H) Hippocampal paired pulse facilitation (two-way ANOVA with Sidak, n = 6-7.

(I) Principal components analysis of all differentially regulated genes from RNA sequencing of CA3 subfields of the hippocampus from GF mice monocolonized with *Clostridium cocleatum* (Clos) or *Bilophila wadsworthia* (Bilo) (n = 6).

(J) Volcano plot labeling genes with high fold change of differential expression (Wald test, n = 6).

(K) Representative image of doublecortin (DCX)-positive neurons in the dentate gyrus (left). Quantitation of DCX density per area of the dentate gyrus (right) (unpaired two-tailed Students t test, n = 4–5). Data are presented as mean ± SEM * p < 0.05, **p < 0.01, ***p < 0.001. n.s., not statistically significant; SPF, specific pathogen-free (conventionally colonized); Abx, treated with antibiotics (ampicillin, vancomycin, metronidazole, and neomycin); GF, germ-free; KD, ketogenic diet; Hyp, intermittent hypoxia exposure; Mock, intermittent normoxia exposure; GF+Clos, GF mice monocolonized with *C. cocleatum*; GF+Bilo; GF mice mono-colonized with *B. wadsworthia*; DCX, doublecortin; LTP, long-term-potentiation; fEPSP, field excitatory post-synaptic potential.

disruptions in hippocampal activity induced by *B. wadsworthia* were comparable with those seen in mice exposed to KD and Hyp, suggesting that colonization with *B. wadsworthia* pheno-copies the adverse effects of KD and Hyp on hippocampal synaptic transmission and plasticity. The microbiota-dependent alterations in hippocampal activity were further associated with microbiota-dependent changes in hippocampal gene expression (Figures S4E–S4J; Table S3). In particular, colonization with *B. wadsworthia* resulted in widespread transcriptomic alterations in the hippocampus relative to *C. cocleatum*-colonized controls (Figure 4I). Particular genes that were differentially ex-

pressed in response to *B. wadsworthia* colonization included subsets related to neuronal excitation (*CBLN1, CC2D1A, GRIK4, SYT2,* and *SYT9*), mitochondrial processes (*DNAJA3, SLC25A16, ALDH4A1,* and *NDUFAF1*), neuronal interactions (*KCNN3, SEMA3C, TTR, MOV10,* and *PLK5*), ubiquitination (*BAP1, COPS6, FBXO4, FBXO42, NDUFAF5,* and *USP53*), and immune response (*LCK, HMGB1, NFKBID, TRAFD1,* and *SPG21*) (Figure 4J). Moreover, immunofluorescence staining for doublecortin (**DCX**), a marker for the central phase of hippo-campal neurogenesis (von Bohlen und Halbach, 2011), revealed reduced density of DCX-positive cells in the dentate gyrus

of mice colonized with *B. wadsworthia* compared with *C. cocleatum*-colonized controls (Figure 4K), adding to prior results demonstrating the microbiota regulates hippocampal neurogenesis (Ogbonnaya et al., 2015). Overall, these results indicate that colonization with *B. wadsworthia* alters hippocampal physiology and further suggest that microbiota-dependent impairments in cognitive behavior may be due, at least in part, to microbiota-dependent disruptions in hippocampal function.

Th1 cell expansion contributes to *Bilophila*-induced impairments in cognitive behavior

B. wadsworthia colonization promotes the expansion of IFNg-producing T helper type I (**Th1**) cells, and IFNg is associated with impairments in cognitive behavior and hippocampal physiology during homeostasis and in response to chronic stress (Devkota et al., 2012; Kim et al., 2011; Litteljohn et al., 2014). We hypothesized that Th1 induction may contribute to the detrimental effects of *B. wadsworthia* and of environmental risk factors, KD and Hyp, on cognitive behavior. To first confirm that *B. wadsworthia* increases Th1 cells, GF mice were monocolonized with either *C. cocleatum* or *B. wadsworthia*, and Th1 levels were measured in the intestine. Indeed, *B. wadsworthia*-colonized mice exhibited increased levels of CD3$^+$CD4$^+$IFNg+IL17a- Th1 cells in the colonic lamina propria relative to GF and *C. cocleatum*-colonized controls (Figures S5A and S5B). Similar increases in levels of Th1 cells were seen by colonization of Abx-treated mice with *B. wadsworthia*, indicating that the Th1-promoting effects of *B. wadsworthia* are observed in response to bacterial enrichment, as well as bacterial monocolonization (Figures S5C and S5D). To determine if Th1 cells are required for the adverse effects of *B. wadsworthia* on cognitive behavior, mice were reared in the absence of Th1 cells (T-bet knockout, **T-bet–/–**) or as genetically wild-type (**WT**) and colonized with *B. wadsworthia* (Figures 5A, S5C, and S5D). Consistent with prior monocolonization experiments conducted with GF Swiss Webster mice (Figure 3), Abx-treated WT C57Bl/6J mice colonized with *B. wadsworthia* exhibited impaired cognitive behavior in the Barnes maze, as denoted by elevated errors made and increased random search strategy relative to noncolonized Abx-treated WT controls (Figures 5B–5F, **Abx+Bilo WT** versus **Abx WT**). In contrast to results from prior monocolonization experiments (Figure 3I), there were no statistically significant differences in latency to enter the escape box (Figure 5C), which may point to effects of *B. wadsworthia* on this particular behavioral parameter that are dependent on bacterial load, prior colonization status, and/or genetic background of the host. Notably, preventing Th1 induction via T-bet deficiency abrogated the adverse effects of *B. wadsworthia* on cognitive behavior, as denoted by reductions in errors made and use of random search strategy to levels comparable with those seen in colonized WT controls (Figures 5D–5F, **Abx+Bilo Tbet–/–** versus **Abx+Bilo WT**). There is no striking difference in latency to enter or errors made in the Barnes maze by Abx-treated Tbet–/– mice relative to WT controls (Figures 5B–5F, **Abx Tbet–/–** versus **Abx WT**), suggesting that the ability of Tbet deficiency to prevent detrimental effects of *B. wadsworthia* colonization are not confounded by baseline impairments in Tbet–/– mice. These results support previous findings that *B. wadsworthia* promotes IFNg-producing Th1 cells in the intestine and further reveal that

Th1 cells are necessary for the ability of *B. wadsworthia* to impair cognitive behavior in mice.

To further determine if Th1 cells contribute to the adverse effects of KD and Hyp on cognitive behavior, mice were reared as T-bet–/– or genetically WT, then exposed to both KD and Hyp (Figure 5G). Consistent with prior experiments using Swiss Webster mice (Figure 1), C57Bl/6J WT SPF mice exposed to both KD and Hyp exhibited impaired performance in the Barnes maze relative to Mock-exposed controls (Figures 5H–5L). Notably, CI induced by KD and Hyp was associated with significant increases in serum IFNg levels (Figure S5G), and modest, but not statistically significant, increases in levels of IFNg-producing Th1 cells in the colonic lamina propria (Figures S5E and S5F). We additionally find that mice exposed to KD and Hyp display elevated levels of serum IL-2 relative to controls (Figure S5H), which may contribute to the increased differentiation of naive CD4$^+$ cells to Th1 cells (Liao et al., 2013). Notably, we observe no differences in levels of classical pro-inflammatory cytokines IL-6, IL-1b, TNFα, KC/GRO, or in regulatory cytokines IL-10 and IL-4 (Figures S5I–S5O), suggesting no evidence of overt inflammation. Inhibiting Th1 induction through T-bet deficiency abrogated the adverse effects of KD and Hyp on cognitive behavior, as denoted by decreases in latency to enter the escape box, errors made, and use of random search strategy, relative to exposed WT controls (Figures 5H–5L). Altogether, these results implicate that *B. wadsworthia* impairs cognitive behavior by increasing IFNg-producing Th1 cells, and further suggest that microbiota-dependent increases in Th1 cells and IFNg contribute to the adverse effects of KD and Hyp on cognitive behavior.

DISCUSSION

Proof-of-concept studies have reported that complete absence or severe depletion of the microbiota results in widespread alterations in complex animal behaviors, including learning and memory (Chu et al., 2019; Desbonnet et al., 2014; Fröhlich et al., 2016; Gareau et al., 2011; Liu et al., 2020; Möhle et al., 2016; Vuong and Hsiao, 2017; Yu et al., 2019). However, whether the microbiota is altered by physiologically relevant risk factors for cognitive dysfunction and whether there are select microbial species that are causally linked to CI has been poorly understood. Results from this study reveal that the gut microbiota is shaped by synergistic interactions between environmental risk factors for CI. They further demonstrate that select diet- and hypoxic stress-responsive bacteria from the gut microbiota disrupt hippocampal function and cognitive behavior, likely via the induction of pro-inflammatory immune cells.

In particular, we find that the high-fat low-carbohydrate KD exacerbates the detrimental effects of acute intermittent Hyp on cognitive behavior. This aligns with the so-called "two-hit" or "multiple-hit" hypotheses for neurological and neurodegenerative diseases (Heinemann et al., 2016), wherein multiple genetic and/or environmental risk factors interact to accelerate or predispose to symptoms of disease, including age-related cognitive decline (Zhu et al., 2007). Indeed, both high-fat diet and hypoxia are associated with CI across studies of humans and animal models (Arias-Cavieres et al., 2020; Beilharz et al., 2015; Jha et al., 2018). However, the KD and select ketone bodies, such as beta-hydroxybutyrate, have been recently explored as
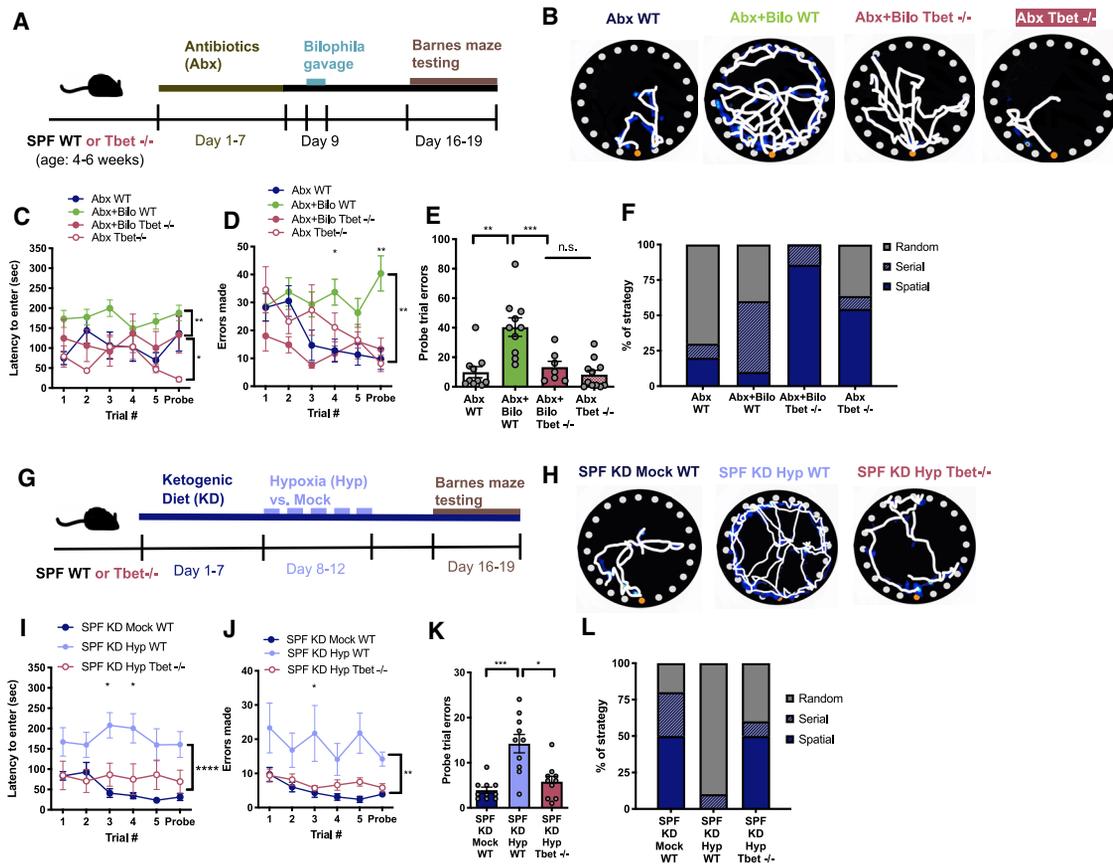
Figure 5. Th1 cell expansion contributes to *bilophila*-induced impairments in cognitive behavior
(A) Experimental timeline.
(B) Representative Barnes maze traces for Abx+WT mice compared with Abx mice colonized with *B. wadsworthia* with either WT or Tbet–/– background. White lines indicate movement trajectories, whereas blue hues denote increasing durations of time spent at a particular location. Orange circles denote the escape hole.
(C) Latency to enter the escape hole (two-way ANOVA with Sidak, n = 7–11).
(D) Errors made (two-way ANOVA with Sidak, n = 7–11).
(E) Errors made during the probe trial (unpaired two-tailed Students t test, n = 7–11).
(F) Search strategy used during the probe trial (n = 7–11).
(G) Experimental timeline.
(H) Representative Barnes maze traces for SPF KD Mock WT mice compared with SPF KD Hyp mice with either WT or Tbet–/– background.
(I) Latency to enter the escape hole (two-way ANOVA with Sidak, n = 10).
(J) Errors made (two-way ANOVA with Sidak, n = 10).
(K) Errors made during the probe trial (unpaired two-tailed Students t test, n = 10).
(L) Search strategy used during the probe trial (n = 10). Data are presented as mean ± SEM *p < 0.05, **p < 0.01. n.s., not statistically significant; SPF, specific pathogen-free (conventionally colonized); Abx (conventionally colonized mice treated with broad-spectrum antibiotics); WT, wild-type; Tbet–/–, knockout line for Tbet transcription factor; KD, ketogenic diet; Mock, intermittent normoxia exposure; Hyp, intermittent hypoxia exposure.

potential treatments for CI with variable results (Fortier et al., 2021; Park et al., 2020; Reger et al., 2004; Zhao et al., 2004). Findings from this study suggest that when combined with other environmental stressors, the KD can be detrimental to hippocampal function and cognitive behavior. This is consistent with one recent report that KD administration in a rat model of Alzheimer's disease worsened cognitive performance in the Morris water maze (Park et al., 2020). Further research is warranted to uncover the molecular bases for interactions between varied genetic and environmental risk factors for CI.

Prior studies have implicated various physiological pathways in mediating the neurological effects of the KD, such as adenosine receptor activation, mitochondrial biogenesis, TCA anaple-

rosis, and altered ion channel expression (Elamin et al., 2020; Masino and Rho, 2012). Data from this study indicate that alterations in the gut microbiota contribute to the ability of the KD to potentiate the adverse effects of Hyp on cognitive behavior in the Barnes maze task. One important consideration is the biological bases of the abnormalities observed in the behavioral task. Adverse effects of the KD and Hyp are seen even during the first trial of the Barnes maze assay that persist through the sixth and last trial. Although we observe no overt differences in stress-induced exploration in the open field, acoustic startle response, and sensorimotor gating in the prepulse inhibition task, the early abnormalities in the Barnes maze suggest that the KD and Hyp together induce cognitive issues that extend beyond disruptions

in spatial learning and working memory. Indeed, depletion of the risk-associated microbiota diminishes the cognitive behavioral abnormalities, even in the first trial of testing, and also improves hippocampal LTP, suggesting that the microbiome may modify hippocampal-dependent learning and memory as well other aspects of cognitive performance. Overall, whereas the data reveal an influence of the gut microbiota in modulating cognitive behavior, the complexity of the behavioral phenotypes leave open the likely possibility that there are multiple microbiota-independent effects of diet and hypoxic stress that also contribute to the observed cognitive phenotypes.

In addition to identifying a synergistic effect of KD and Hyp on impairing cognitive behavior, we also reveal an interaction between KD and Hyp in enriching *Bilophila* species in the gut microbiota. Although the exact mechanisms remain unknown, one study reported particular alterations in the gut microbiota that were seen when rats were exposed to both the high-fat, high-sugar diet, and hypoxia in a model of obstructive sleep apnea (**OSA**) (Durgan et al., 2016). A separate paper studying intermittent hypoxia as a model of OSA found that fecal microbiome transplantation of hypoxia-associated samples sufficiently promoted murine sleep disturbances and that the microbial family *Desulfovibrionaceae* (OTU147), which *Bilophila* is a member of, was increased in hypoxia-associated samples and in children with OSA (Badran et al., 2020; Valentini et al., 2020). In a similar paradigm where atherosclerosis-prone *Ldlr-/-* mice were fed a high-fat diet, additional exposure to hypoxia and hypercapnia increased levels of select bile acids, particularly taurodeoxycholic acid (Tripathi et al., 2018).This may be relevant, as a separate study reported that a high-saturated fat diet promoted taurine conjugation of bile acids, and that taurocholic acid in particular promoted levels of *B. wadsworthia* in mice (Devkota et al., 2012). Based on these studies and the finding that *B. wadsworthia* is an obligate anaerobe (Devkota et al., 2012; Summanen et al., 1995), we speculate that the KD and Hyp together enrich *Bilophila* through combined modulation of bile acid profiles and increased anaerobicity of the intestinal microenvironment. Future co-culture and metabolic modeling experiments are needed to dissect how various environmental factors differentially influence microbial community structures.

Consistent with the finding that KD and Hyp together impair cognitive behavior and enrich *Bilophila* in the gut microbiota, we observe that colonization with *B. wadsworthia* leads to disrupted hippocampal physiology and cognitive deficits. These findings align with studies linking *B. wadsworthia* to increases in IFNg (Devkota et al., 2012), and separately, to increases in IFNg to CI (Monteiro et al., 2016). Although the molecular mechanisms by which *Bilophila* stimulates Th1 cell expansion remain unclear, prior research reported that lysates from *Bilophila* cultures are sufficient induce Th1 cell proliferation and IFNg production, as well as IL-12 production by dendritic cells (Devkota et al., 2012). These data suggest that acute exposure to molecular factors derived from *Bilophila* stimulate IL-12 from dendritic cells, which drives Th1 cell expansion (Devkota et al., 2012). Future advancements and continued research are needed to clearly identify the bacterial factors that enable *Bilophila* to stimulate IFNg-producing Th1 cells and CI.

Notably, whereas results from our study highlight a likely role for *Bilophila* in contributing to environmental risk for CI (as induced by KD and Hyp in mice), they do not the preclude the possibility that other members of the microbiota may also modify cognitive behavior. In particular, 16S rRNA gene sequences from *Bilophila* are reported to comprise approximately 0.004%–0.3% of 16S rRNA loads from the fecal microbiota of SPF mice (Caesar et al., 2015). In our experiments, KD and Hyp together (but not individually) increase the absolute abundance of *Bilophila* 16S rRNA gene copies in feces by ~1000X. As such, the physiological loads of *B. wadsworthia* in the presence of a complex SPF microbiota, even after increases seen in response to KD and Hyp, are much lower than those achieved by subsequent experiments involving bacterial monocolonization of GF mice or enrichment in Abx-treated mice. Results from our study indicate that gnotobiotic colonization with *B. wadsworthia* largely phenocopies the cognitive behavioral impairment, hippocampal dysfunction, and Th1 induction seen in response to KD and Hyp (and their associated physiological increases in *Bilophila*). Although we did not observe other bacterial taxa, aside from *Bilophila*, that were significantly elevated in response to both KD and Hyp, future studies of various risk factors for CI may reveal additional microbial taxa and signaling pathways that modify hippocampal function and cognitive behavior.

Consistent with previous literature indicating that *B. wadsworthia* promotes Th1 cell expansion (Devkota et al., 2012), we observe that T-bet deficiency prevents *B. wadsworthia*-induced increases in IFNg-producing Th1 cells, as well as the cognitive behavioral impairments seen in *B. wadsworthia*-colonized mice. Precisely how IFNg-producing Th1 cells promote cognitive behavioral abnormalities remains poorly understood. However, increases in Th1 cells and Th1 responses are commonly associated with aging-associated cognitive decline and CI in Alzheimer's disease (Browne et al., 2013; Dulken et al., 2019). Moreover, prior literature reports that IFNg and its receptor (**IFNGR**) are necessary for mediating memory impairment in mice (Monteiro et al., 2016; Zhang et al., 2020), and that IFNg is sufficient to drive hippocampal dysfunction and abnormal cognitive behavior in mice (Zhang et al., 2020). IFNg applied to hippocampal slices reduces gamma oscillations, which are critical to higher brain functioning and may be one explanation for how *Bilophila* manipulates hippocampal activity (Colgin and Moser, 2010; Ta et al., 2019). IL-4, which suppresses Th1 cell differentiation, also alters cognitive function (Derecki et al., 2010; Zhang et al., 2020). The precise signaling mechanisms remain unclear as both neurons and microglia are known to express IFNGR and respond to IFNg (Mizuno et al., 2008; Zhang et al., 2020). IFNg production by Th1 cells promotes microglial activation (Mount et al., 2007; Takeuchi et al., 2006; Zhou et al., 2015) and hippocampal-dependent cognitive dysfunction (Litteljohn et al., 2014; Monteiro et al., 2016; Zhang et al., 2020). One study reported that IFNg induces neurotoxicity by reducing neuronal ATP production via IFNg-mediated GluR1 phosphorylation (Mizuno et al., 2008). IFNg is also reported to have the capacity to increase blood-brain barrier permeability (Rahman et al., 2018). In addition to direct effects of IFNg in the brain, peripheral IFNg may act through as yet unknown indirect mechanisms to impact central neurocircuits underlying cognitive function. Peripheral and hippocampal IFNg corresponds with impaired Barnes maze performance due to chronic mild stress (Palumbo et al., 2018). In aged murine brains, T cell

Cell Host & Microbe
Article

CellPress

infiltration occurs in neurogenic niches and IFNg correlates with reduced neural stem cell function and proliferation (Dulken et al., 2019). Indeed, IFNg directly suppresses hippocampal neural stem/precursor cell proliferation and provokes neuronal apoptosis (Zhang et al., 2020). *B. wadsworthia* has also been identified in several human microbiome association studies as associating with aging (Shenghua et al., 2020) and aging-associated neurodegenerative disorders (Baldini et al., 2020; Lin et al., 2019; Vogt et al., 2017). Further studies are needed to determine how microbiota-dependent neuroimmune interactions may influence cognitive health.

As the prevalence of cognitive dysfunction continues to increase (Hale et al., 2020), identifying early and modifiable risk factors is critical to enabling early detection and intervention for CI. Results from this study reveal that the gut microbiota is altered by modeling select environmental risk factors for CI in mice and that changes in the gut microbiota, and *Bilophila* in particular, contribute to disruptions in hippocampal physiology and cognitive behavior. We propose that understanding the biological bases for how complex genetic, environmental, and psychosocial factors together predispose to CI requires consideration of the gut microbiome, as an important interface between host genetics and environmental exposures and an integral regulator of nutrition, immunity, metabolism, and behavior.

Limitations of study
Foundational prior research has revealed that the absence or depletion of the gut microbiota in rodents results in abnormalities in learning and memory across various behavioral paradigms (Chu et al., 2019; Desbonnet et al., 2014; Fröhlich et al., 2016; Gareau et al., 2011; Liu et al., 2020; Möhle et al., 2016; Vuong and Hsiao, 2017; Yu et al., 2019). Herein, we extend these works by modeling two environmental factors for CI—the high-fat low-carbohydrate KD and intermittent hypoxia. We find that that these particular environmental factors interact to elicit select alterations in the gut microbiota. Furthermore, we find that these changes in the complex gut microbiota, which are characterized by increases in *Bilophila* in our particular study, contribute to hippocampal dysfunction and impaired cognitive behavior in the Barnes maze. Notably, mouse KDs with varying fat to carbohydrate ratios have been used in the existing literature with similar effects on host phenotypes such as behavior and neurotransmission but can also show some nuanced differences (Murphy et al., 2005; Ruskin et al., 2017). We implemented one common form of the mouse KD, based on prior studies (Olson et al., 2018; Samala et al., 2008). In addition, a wide range of hypoxia regimens have been reported to induce varying degrees of CI in mice (Deguil et al., 2016), and this study employs only one version of intermittent hypoxia (12% oxygen, 6 h per day for 5 days) followed by one spatial learning and memory task—the Barnes maze—at 4–7 days after the last day of hypoxia exposure. Importantly, this study models pre-exposure to the KD followed by challenge with Hyp, and finds that consumption of the KD exacerbates Hyp-induced CI in mice. Additional research is needed to determine if temporal differences in KD consumption would yield different results and in particular, to assess effects of the KD when supplied after Hyp exposure. Overall, whether the findings in this study will be generalizable across all variations of KD and hypoxia regimens and all cognitive behavioral paradigms in mice remains to be tested.

Similarly, we observe that *Bilophila* is enriched by the KD and hypoxia regimen used in this study, which aligns with reported increases in *B. wadsworthia* in response to high-fat diet and elevations in taurocholic acid (Devkota et al., 2012; Summanen et al., 1995). This evidence suggests that KD- and Hyp-induced changes in bile acid metabolism and anaerobicity of the intestinal microenvironment may be responsible for enriching *Bilophila*. However, microbiota composition is known to vary across species, backgrounds, vendors, facilities, cages, sexes, and ages, among many other factors, raising the question of whether KD- and Hyp-induced enrichment of *Bilophila* in particular will be seen universally despite variations in the composition of the SPF mouse microbiota. Nonetheless, we find that monocolonization with or enrichment of *B. wadsworthia* alone impairs hippocampal function and cognitive behavior in mice. This suggests that the findings herein may be relevant to other environmental risk factors or conditions that elevate *B. wadsworthia*.

Despite the caveats regarding the particular parameters used for KD, Hyp, SPF microbiota, and behavioral testing, we find that *B. wadsworthia* colonization impairs hippocampal LTP, gene expression and markers of neurogenesis, as well as cognitive behavior in the Barnes maze, in a manner that is dependent upon IFNg-producing Th1 cells. This aligns with existing literature linking IFNg and Th1 induction to abnormalities in hippocampal physiology, learning, memory, and cognition (Litteljohn et al., 2014; Monteiro et al., 2016; Zhang et al., 2020). Altogether, these findings support a role for microbiota-induced pro-inflammatory responses in contributing to brain and behavioral endophenotypes of CI.

STAR★METHODS

Detailed methods are provided in the online version of this paper and include the following:

- KEY RESOURCES TABLE
- RESOURCE AVAILABILITY
  - Lead contact
  - Materials availability
  - Data and code availability
- EXPERIMENTAL MODELS AND SUBJECT DETAILS
  - Mice
  - Bacteria
- METHOD DETAILS
  - Dietary treatment
  - Acute intermittent hypoxia
  - Barnes maze testing
  - Open field testing
  - Prepulse inhibition testing
  - Antibiotic treatment
  - Fecal microbiota transplant
  - 16S rRNA gene sequencing
  - Gnotobiotic colonization and antibiotic enrichment
  - Hippocampal electrophysiology
  - Hippocampal transcriptomic profiling
  - Hippocampal immunofluorescence staining and imaging
  - Lymphocyte isolation and flow cytometry

○ Digital PCR
○ Serum cytokine quantification
● QUANTIFICATION AND STATISTICAL ANALYSIS

SUPPLEMENTAL INFORMATION

Supplemental information can be found online at https://doi.org/10.1016/j.chom.2021.07.004.

AUTHOR CONTRIBUTIONS

C.A.O., A.J.I., G.E.Y., P.F., G.N.P., K.G.J, and J.T.B.performed the experiments and analyzed the data. C.A.O., A.J.I., R.F.I., and E.Y.H. designed the study. C.A.O. and E.Y.H wrote the manuscript. All authors discussed the results and commented on the manuscript.

DECLARATION OF INTERESTS

The authors declare no competing interests.

INCLUSION AND DIVERSITY

We worked to ensure sex balance in the selection of non-human subjects. One or more of the authors of this paper self-identifies as an underrepresented ethnic minority in science. While citing references scientifically relevant for this work, we also actively worked to promote gender balance in our reference list.

REFERENCES

Akinyemi, R.O., Mukaetova-Ladinska, E.B., Attems, J., Ihara, M., and Kalaria, R.N. (2013). Vascular risk factors and neurodegeneration in ageing related dementias: Alzheimer's disease and vascular dementia. Curr. Alzheimer Res. *10*, 642–653.

Amir, A., McDonald, D., Navas-Molina, J.A., Kopylova, E., Morton, J.T., Zech Xu, Z., Kightley, E.P., Thompson, L.R., Hyde, E.R., Gonzalez, A., and Knight, R. (2017). Deblur rapidly resolves single-nucleotide community sequence patterns. mSystems *2*.

Anders, S., Pyl, P.T., and Huber, W. (2015). HTSeq–a Python framework to work with high-throughput sequencing data. Bioinformatics *31*, 166–169.

Andrews, S. (2010). FastQC: a quality control tool for high throughput sequence data. http://www.bioinformatics.babraham.ac.uk/projects/fastqc.

Arcego, D.M., Toniazzo, A.P., Krolow, R., Lampert, C., Berlitz, C., Dos Santos Garcia, E., do Couto Nicola, F., Hoppe, J.B., Gaelzer, M.M., Klein, C.P., et al. (2018). Impact of high-fat diet and early stress on depressive-like behavior and hippocampal plasticity in adult male rats. Mol. Neurobiol. *55*, 2740–2753.

Arias-Cavieres, A., Khuu, M.A., Nwakudu, C.U., Barnard, J.E., Dalgin, G., and Garcia, A.J., 3rd. (2020). A HIF1a-dependent pro-oxidant state disrupts synaptic plasticity and impairs spatial memory in response to intermittent hypoxia. eNeuro *7*.

Attar, A., Liu, T., Chan, W.T., Hayes, J., Nejad, M., Lei, K., and Bitan, G. (2013). A shortened Barnes maze protocol reveals memory deficits at 4-months of age in the triple-transgenic mouse model of Alzheimer's disease. PloS One *8*, e80355.

Aubrecht, T.G., Jenkins, R., Magalang, U.J., and Nelson, R.J. (2015). Influence of gonadal hormones on the behavioral effects of intermittent hypoxia in mice. Am. J. Physiol. Regul. Integr. Comp. Physiol. *308*, R489–R499.

Babiec, W.E., Jami, S.A., Guglietta, R., Chen, P.B., and O'Dell, T.J. (2017). Differential regulation of NMDA receptor-mediated transmission by SK channels underlies dorsal-ventral differences in dynamics of Schaffer collateral synaptic function. J. Neurosci. *37*, 1950–1964.

Badran, M., Khalyfa, A., Ericsson, A., and Gozal, D. (2020). Fecal microbiota transplantation from mice exposed to chronic intermittent hypoxia elicits sleep disturbances in naïve mice. Exp. Neurol. *334*, 113439.

Bahr, L.S., Bock, M., Liebscher, D., Bellmann-Strobl, J., Franz, L., Prüß, A., Schumann, D., Piper, S.K., Kessler, C.S., Steckhan, N., et al. (2020). Ketogenic diet and fasting diet as Nutritional Approaches in Multiple Sclerosis (NAMS): protocol of a randomized controlled study. Trials *21*, 3.

Baldini, F., Hertel, J., Sandt, E., Thinnes, C.C., Neuberger-Castillo, L., Pavelka, L., Betsou, F., Krüger, R., and Thiele, I.; NCER-PD Consortium (2020). Parkinson's disease-associated alterations of the gut microbiome predict disease-relevant changes in metabolic functions. BMC Biol *18*, 62.

Beilharz, J.E., Maniam, J., and Morris, M.J. (2015). Diet-induced cognitive deficits: the role of fat and sugar, potential mechanisms and nutritional interventions. Nutrients *7*, 6719–6738.

Biswal, S., Sharma, D., Kumar, K., Nag, T.C., Barhwal, K., Hota, S.K., and Kumar, B. (2016). Global hypoxia induced impairment in learning and spatial memory is associated with precocious hippocampal aging. Neurobiol. Learn. Mem. *133*, 157–170.

Bolger, A.M., Lohse, M., and Usadel, B. (2014). Trimmomatic: a flexible trimmer for Illumina sequence data. Bioinformatics *30*, 2114–2120.

Bolyen, E., Rideout, J.R., Dillon, M.R., Bokulich, N.A., Abnet, C.C., Al-Ghalith, G.A., Alexander, H., Alm, E.J., Arumugam, M., Asnicar, F., et al. (2019). Reproducible, interactive, scalable and extensible microbiome data science using QIIME 2. Nat. Biotechnol. *37*, 852–857.

Bravo, J.A., Forsythe, P., Chew, M.V., Escaravage, E., Savignac, H.M., Dinan, T.G., Bienenstock, J., and Cryan, J.F. (2011). Ingestion of Lactobacillus strain regulates emotional behavior and central GABA receptor expression in a mouse via the vagus nerve. Proc. Natl. Acad. Sci. USA *108*, 16050–16055.

Browne, T.C., McQuillan, K., McManus, R.M., O'Reilly, J.A., Mills, K.H., and Lynch, M.A. (2013). IFN-γ production by amyloid β-specific Th1 cells promotes microglial activation and increases plaque burden in a mouse model of Alzheimer's disease. J. Immunol. *190*, 2241–2251.

Buffington, S.A., Di Prisco, G.V., Auchtung, T.A., Ajami, N.J., Petrosino, J.F., and Costa-Mattioli, M. (2016). Microbial reconstitution reverses maternal diet-induced social and synaptic deficits in offspring. Cell *165*, 1762–1775.

Caesar, R., Tremaroli, V., Kovatcheva-Datchary, P., Cani, P.D., and Bäckhed, F. (2015). Crosstalk between gut microbiota and dietary lipids aggravates WAT inflammation through TLR signaling. Cell Metab *22*, 658–668.

Caporaso, J.G., Lauber, C.L., Walters, W.A., Berg-Lyons, D., Lozupone, C.A., Turnbaugh, P.J., Fierer, N., and Knight, R. (2011). Global patterns of 16S rRNA

Cell Host & Microbe
Article

CellPress

diversity at a depth of millions of sequences per sample. Proc. Natl. Acad. Sci. USA *108* (suppl 1), 4516–4522.

Chu, C., Murdock, M.H., Jing, D., Won, T.H., Chung, H., Kressel, A.M., Tsaava, T., Addorisio, M.E., Putzel, G.G., Zhou, L., et al. (2019). The microbiota regulate neuronal function and fear extinction learning. Nature *574*, 543–548.

Colgin, L.L., and Moser, E.I. (2010). Gamma oscillations in the hippocampus. Physiology (Bethesda) *25*, 319–329.

Cordner, Z.A., and Tamashiro, K.L. (2015). Effects of high-fat diet exposure on learning & memory. Physiol. Behav. *152*, 363–371.

D'Amato, A., Di Cesare Mannelli, L., Lucarini, E., Man, A.L., Le Gall, G., Branca, J.J.V., Ghelardini, C., Amedei, A., Bertelli, E., Regoli, M., et al. (2020). Faecal microbiota transplant from aged donor mice affects spatial learning and memory via modulating hippocampal synaptic plasticity- and neurotransmission-related proteins in young recipients. Microbiome *8*, 140.

Das, S.K., Dhar, P., Sharma, V.K., Barhwal, K., Hota, S.K., Norboo, T., and Singh, S.B. (2018). High altitude with monotonous environment has significant impact on mood and cognitive performance of acclimatized lowlanders: possible role of altered serum BDNF and plasma homocysteine level. J. Affect. Disord. *237*, 94–103.

David, L.A., Maurice, C.F., Carmody, R.N., Gootenberg, D.B., Button, J.E., Wolfe, B.E., Ling, A.V., Devlin, A.S., Varma, Y., Fischbach, M.A., et al. (2014). Diet rapidly and reproducibly alters the human gut microbiome. Nature *505*, 559–563.

de Aquino Lemos, V., Antunes, H.K., dos Santos, R.V., Lira, F.S., Tufik, S., and de Mello, M.T. (2012). High altitude exposure impairs sleep patterns, mood, and cognitive functions. Psychophysiology *49*, 1298–1306.

Deguil, J., Ravasi, L., Lanteaume, L., Lamberty, Y., and Bordet, R. (2016). Translational challenge models in support of efficacy studies: effect of cerebral hypoxia on cognitive performances in rodents. CNS Neurol. Disord. Drug Targets *15*, 765–776.

Derecki, N.C., Cardani, A.N., Yang, C.H., Quinnies, K.M., Crihfield, A., Lynch, K.R., and Kipnis, J. (2010). Regulation of learning and memory by meningeal immunity: a key role for IL-4. J. Exp. Med. *207*, 1067–1080.

Desbonnet, L., Clarke, G., Shanahan, F., Dinan, T.G., and Cryan, J.F. (2014). Microbiota is essential for social development in the mouse. Mol. Psychiatry *19*, 146–148.

Devkota, S., Wang, Y., Musch, M.W., Leone, V., Fehlner-Peach, H., Nadimpalli, A., Antonopoulos, D.A., Jabri, B., and Chang, E.B. (2012). Dietary-fat-induced taurocholic acid promotes pathobiont expansion and colitis in Il10-/- mice. Nature *487*, 104–108.

Dulken, B.W., Buckley, M.T., Navarro Negredo, P., Saligrama, N., Cayrol, R., Leeman, D.S., George, B.M., Boutet, S.C., Hebestreit, K., Pluvinage, J.V., et al. (2019). Single-cell analysis reveals T cell infiltration in old neurogenic niches. Nature *571*, 205–210.

Duncombe, J., Kitamura, A., Hase, Y., Ihara, M., Kalaria, R.N., and Horsburgh, K. (2017). Chronic cerebral hypoperfusion: a key mechanism leading to vascular cognitive impairment and dementia. Closing the translational gap between rodent models and human vascular cognitive impairment and dementia. Clin. Sci. (Lond.) *131*, 2451–2468.

Durgan, D.J., Ganesh, B.P., Cope, J.L., Ajami, N.J., Phillips, S.C., Petrosino, J.F., Hollister, E.B., and Bryan, R.M., Jr. (2016). Role of the gut microbiome in obstructive sleep apnea-induced hypertension. Hypertension *67*, 469–474.

Dutton, S.B., Sawyer, N.T., Kalume, F., Jumbo-Lucioni, P., Borges, K., Catterall, W.A., and Escayg, A. (2011). Protective effect of the ketogenic diet in Scn1a mutant mice. Epilepsia *52*, 2050–2056.

Elamin, M., Ruskin, D.N., Sacchetti, P., and Masino, S.A. (2020). A unifying mechanism of ketogenic diet action: the multiple roles of nicotinamide adenine dinucleotide. Epilepsy Res *167*, 106469.

Fortier, M., Castellano, C.A., St-Pierre, V., Myette-Côté, É., Langlois, F., Roy, M., Morin, M.C., Bocti, C., Fulop, T., Godin, J.-P., et al. (2021). A ketogenic drink improves cognition in mild cognitive impairment: results of a 6-month RCT. Alzheimers Dement *17*, 543–552.

Fröhlich, E.E., Farzi, A., Mayerhofer, R., Reichmann, F., Jačan, A., Wagner, B., Zinser, E., Bordag, N., Magnes, C., Fröhlich, E., et al. (2016). Cognitive impairment by antibiotic-induced gut dysbiosis: analysis of gut microbiota-brain communication. Brain Behav. Immun. *56*, 140–155.

Gareau, M.G., Wine, E., Rodrigues, D.M., Cho, J.H., Whary, M.T., Philpott, D.J., Macqueen, G., and Sherman, P.M. (2011). Bacterial infection causes stress-induced memory dysfunction in mice. Gut *60*, 307–317.

Giuliani, A., Sivilia, S., Baldassarro, V.A., Gusciglio, M., Lorenzini, L., Sannia, M., Calzà, L., and Giardino, L. (2019). Age-related changes of the neurovascular unit in the cerebral cortex of Alzheimer disease mouse models: a neuroanatomical and molecular study. J. Neuropathol. Exp. Neurol. *78*, 101–112.

Goldbart, A.D., Row, B.W., Kheirandish-Gozal, L., Cheng, Y., Brittian, K.R., and Gozal, D. (2006). High fat/refined carbohydrate diet enhances the susceptibility to spatial learning deficits in rats exposed to intermittent hypoxia. Brain Res *1090*, 190–196.

Gozal, E., Gozal, D., Pierce, W.M., Thongboonkerd, V., Scherzer, J.A., Sachleben, L.R., Jr., Brittian, K.R., Guo, S.Z., Cai, J., and Klein, J.B. (2002). Proteomic analysis of CA1 and CA3 regions of rat hippocampus and differential susceptibility to intermittent hypoxia. J. Neurochem. *83*, 331–345.

Hale, J.M., Schneider, D.C., Gampe, J., Mehta, N.K., and Myrskylä, M. (2020). Trends in the risk of cognitive impairment in the United States, 1996–2014. Epidemiology *31*, 745–754.

Han, B., Chen, H., Yao, Y., Liu, X., Nie, C., Min, J., Zeng, Y., and Lutz, M.W. (2020). Genetic and non-genetic factors associated with the phenotype of exceptional longevity & normal cognition. Sci. Rep. *10*, 19140.

Heinemann, S.D., Posimo, J.M., Mason, D.M., Hutchison, D.F., and Leak, R.K. (2016). Synergistic stress exacerbation in hippocampal neurons: evidence favoring the dual-hit hypothesis of neurodegeneration. Hippocampus *26*, 980–994.

Hoban, A.E., Moloney, R.D., Golubeva, A.V., McVey Neufeld, K.A., O'Sullivan, O., Patterson, E., Stanton, C., Dinan, T.G., Clarke, G., and Cryan, J.F. (2016). Behavioural and neurochemical consequences of chronic gut microbiota depletion during adulthood in the rat. Neuroscience *339*, 463–477.

Hsiao, E.Y. (2013). Immune dysregulation in autism spectrum disorder. Int. Rev. Neurobiol. *113*, 269–302.

Hsiao, E.Y., McBride, S.W., Hsien, S., Sharon, G., Hyde, E.R., McCue, T., Codelli, J.A., Chow, J., Reisman, S.E., Petrosino, J.F., et al. (2013). Microbiota modulate behavioral and physiological abnormalities associated with neurodevelopmental disorders. Cell *155*, 1451–1463.

Huang, da W., Sherman, B.T., and Lempicki, R.A. (2009a). Bioinformatics enrichment tools: paths toward the comprehensive functional analysis of large gene lists. Nucleic Acids Res *37*, 1–13.

Huang, da W., Sherman, B.T., and Lempicki, R.A. (2009b). Systematic and integrative analysis of large gene lists using DAVID bioinformatics resources. Nat. Protoc. *4*, 44–57.

Jha, N.K., Jha, S.K., Sharma, R., Kumar, D., Ambasta, R.K., and Kumar, P. (2018). Hypoxia-induced signaling activation in neurodegenerative diseases: targets for new therapeutic strategies. J. Alzheimers. Dis. *62*, 15–38.

Kanoski, S.E., and Davidson, T.L. (2011). Western diet consumption and cognitive impairment: links to hippocampal dysfunction and obesity. Physiol. Behav. *103*, 59–68.

Kanoski, S.E., Zhang, Y., Zheng, W., and Davidson, T.L. (2010). The effects of a high-energy diet on hippocampal function and blood-brain barrier integrity in the rat. J. Alzheimers. Dis. *21*, 207–219.

Kesby, J.P., Kim, J.J., Scadeng, M., Woods, G., Kado, D.M., Olefsky, J.M., Jeste, D.V., Achim, C.L., and Semenova, S. (2015). Spatial cognition in adult and aged mice exposed to high-fat diet. PLoS One *10*, e0140034.

Kim, S.J., Lee, H., Joung, H.Y., Lee, G., Lee, H.J., Shin, M.K., Kim, S.H., Shim, I., and Bae, H. (2011). T-bet deficient mice exhibit resistance to stress-induced development of depression-like behaviors. Journal of neuroimmunology *240-241*, 45–51.

Kim, D., Paggi, J.M., Park, C., Bennett, C., and Salzberg, S.L. (2019). Graph-based genome alignment and genotyping with HISAT2 and HISAT-genotype. Nat. Biotechnol. *37*, 907–915.

Kolde, R. (2015). pheatmap: Pretty heatmaps. ftp://cran.r-project.org/pub/R/web/packages/pheatmap/pheatmap.pdf.

Lauritzen, K.H., Hasan-Olive, M.M., Regnell, C.E., Kleppa, L., Scheibye-Knudsen, M., Gjedde, A., Klungland, A., Bohr, V.A., Storm-Mathisen, J., and Bergersen, L.H. (2016). A ketogenic diet accelerates neurodegeneration in mice with induced mitochondrial DNA toxicity in the forebrain. Neurobiol. Aging 48, 34–47.

Lein, E.S., Hawrylycz, M.J., Ao, N., Ayres, M., Bensinger, A., Bernard, A., Boe, A.F., Boguski, M.S., Brockway, K.S., Byrnes, E.J., et al. (2007). Genome-wide atlas of gene expression in the adult mouse brain. Nature 445, 168–176.

Li, X., Redus, L., Chen, C., Martinez, P.A., Strong, R., Li, S., and O'Connor, J.C. (2013). Cognitive dysfunction precedes the onset of motor symptoms in the MitoPark mouse model of Parkinson's disease. PloS one 8, e71341.

Liao, W., Lin, J.X., and Leonard, W.J. (2013). Interleukin-2 at the crossroads of effector responses, tolerance, and immunotherapy. Immunity 38, 13–25.

Lin, C.-H., Chen, C.-C., Chiang, H.-L., Liou, J.-M., Chang, C.-M., Lu, T.-P., Chuang, E.Y., Tai, Y.C., Cheng, C., Lin, H.Y., et al. (2019). Altered gut microbiota and inflammatory cytokine responses in patients with Parkinson's disease. J. Neuroinflammation 16, 129.

Litteljohn, D., Nelson, E., and Hayley, S. (2014). IFN-γ differentially modulates memory-related processes under basal and chronic stressor conditions. Front. Cell. Neurosci. 8, 391.

Liu, Z., Dai, X., Zhang, H., Shi, R., Hui, Y., Jin, X., Zhang, W., Wang, L., Wang, Q., Wang, D., et al. (2020). Gut microbiota mediates intermittent-fasting alleviation of diabetes-induced cognitive impairment. Nat. Commun. 11, 855.

Lobionda, S., Sittipo, P., Kwon, H.Y., and Lee, Y.K. (2019). The role of gut microbiota in intestinal inflammation with respect to diet and extrinsic stressors. Microorganisms 7, 271.

Love, M.I., Huber, W., and Anders, S. (2014). Moderated estimation of fold change and dispersion for RNA-seq data with DESeq2. Genome Biol 15, 550.

Marques, T.M., Wall, R., Ross, R.P., Fitzgerald, G.F., Ryan, C.A., and Stanton, C. (2010). Programming infant gut microbiota: influence of dietary and environmental factors. Curr. Opin. Biotechnol. 21, 149–156.

Masino, S.A., and Rho, J.M. (2012). Mechanisms of ketogenic diet action. In Jasper's Basic Mechanisms of the Epilepsies, J.L. Noebels, M. Avoli, M.A. Rogawski, R.W. Olsen, and A.V. Delgado-Escueta, eds. (National Center for Biotechnology Information), pp. 1483–1516.

Mavrodaris, A., Powell, J., and Thorogood, M. (2013). Prevalences of dementia and cognitive impairment among older people in sub-Saharan Africa: a systematic review. Bull. World Health Organ. 91, 773–783.

McDonald, T.J.W., and Cervenka, M.C. (2019). Lessons learned from recent clinical trials of ketogenic diet therapies in adults. Curr. Opin. Clin. Nutr. Metab. Care 22, 418–424.

Mei, X., Tan, G., and Qing, W. (2020). AMPK activation increases postoperative cognitive impairment in intermittent hypoxia rats via direct activating PAK2. Behav. Brain Res. 379, 112344.

Mizuno, T., Zhang, G., Takeuchi, H., Kawanokuchi, J., Wang, J., Sonobe, Y., Jin, S., Takada, N., Komatsu, Y., and Suzumura, A. (2008). Interferon-gamma directly induces neurotoxicity through a neuron specific, calcium-permeable complex of IFN-gamma receptor and AMPA GluR1 receptor. FASEB J 22, 1797–1806.

Möhle, L., Mattei, D., Heimesaat, M.M., Bereswill, S., Fischer, A., Alutis, M., French, T., Hambardzumyan, D., Matzinger, P., Dunay, I.R., and Wolf, S.A. (2016). Ly6C(hi) monocytes provide a link between antibiotic-induced changes in gut microbiota and adult hippocampal neurogenesis. Cell Rep 15, 1945–1956.

Monteiro, S., Ferreira, F.M., Pinto, V., Roque, S., Morais, M., de Sá-Calçada, D., Mota, C., Correia-Neves, M., and Cerqueira, J.J. (2016). Absence of IFNγ promotes hippocampal plasticity and enhances cognitive performance. Transl. Psychiatry 6, e707.

Mount, M.P., Lira, A., Grimes, D., Smith, P.D., Faucher, S., Slack, R., Anisman, H., Hayley, S., and Park, D.S. (2007). Involvement of interferon-gamma in microglial-mediated loss of dopaminergic neurons. J. Neurosci. 27, 3328–3337.

Murphy, P., Likhodii, S.S., Hatamian, M., and McIntyre Burnham, W. (2005). Effect of the ketogenic diet on the activity level of Wistar rats. Pediatr. Res. 57, 353–357.

Nagpal, R., Neth, B.J., Wang, S., Craft, S., and Yadav, H. (2019). Modified Mediterranean-ketogenic diet modulates gut microbiome and short-chain fatty acids in association with Alzheimer's disease markers in subjects with mild cognitive impairment. EBioMedicine 47, 529–542.

Noble, E.E., Hsu, T.M., and Kanoski, S.E. (2017). Gut to brain dysbiosis: mechanisms linking Western diet consumption, the microbiome, and cognitive impairment. Front. Behav. Neurosci. 11, 9.

Ogbonnaya, E.S., Clarke, G., Shanahan, F., Dinan, T.G., Cryan, J.F., and O'Leary, O.F. (2015). Adult hippocampal neurogenesis is regulated by the microbiome. Biol. Psychiatry 78, e7–e9.

Olson, C.A., Vuong, H.E., Yano, J.M., Liang, Q.Y., Nusbaum, D.J., and Hsiao, E.Y. (2018). The gut microbiota mediates the anti-seizure effects of the ketogenic diet. Cell 173, 1728–1741.e13.

Ota, M., Matsuo, J., Ishida, I., Takano, H., Yokoi, Y., Hori, H., Yoshida, S., Ashida, K., Nakamura, K., Takahashi, T., and Kunugi, H. (2019). Effects of a medium-chain triglyceride-based ketogenic formula on cognitive function in patients with mild-to-moderate Alzheimer's disease. Neurosci. Lett. 690, 232–236.

O'Toole, P.W., and Jeffery, I.B. (2015). Gut microbiota and aging. Science 350, 1214–1215.

Palumbo, M.L., Di Rosso, M.E., Simon, E.H., Gonzalez Murano, M.R., and Genaro, A.M. (2018). Altered interferon-γ expression in lymphocytes as a potential peripheral marker of chronic stress-induced cognitive deficit. Cytokine 107, 26–34.

Park, S., Zhang, T., Wu, X., and Yi Qiu, J. (2020). Ketone production by ketogenic diet and by intermittent fasting has different effects on the gut microbiota and disease progression in an Alzheimer's disease rat model. J. Clin. Biochem. Nutr. 67, 188–198.

Phillips, M.C.L., Murtagh, D.K.J., Gilbertson, L.J., Asztely, F.J.S., and Lynch, C.D.P. (2018). Low-fat versus ketogenic diet in Parkinson's disease: a pilot randomized controlled trial. Mov. Disord. 33, 1306–1314.

Pistell, P.J., Morrison, C.D., Gupta, S., Knight, A.G., Keller, J.N., Ingram, D.K., and Bruce-Keller, A.J. (2010). Cognitive impairment following high fat diet consumption is associated with brain inflammation. J. Neuroimmunol. 219, 25–32.

Pun, M., Guadagni, V., Drogos, L.L., Pon, C., Hartmann, S.E., Furian, M., Lichtblau, M., Muralt, L., Bader, P.R., Moraga, F.A., et al. (2019). Cognitive effects of repeated acute exposure to very high altitude among altitude-experienced workers at 5050 m. High Alt. Med. Biol. 20, 361–374.

Qaid, E., Zakaria, R., Sulaiman, S.F., Yusof, N.M., Shafin, N., Othman, Z., Ahmad, A.H., and Aziz, C.A. (2017). Insight into potential mechanisms of hypobaric hypoxia-induced learning and memory deficit - Lessons from rat studies. Hum. Exp. Toxicol. 36, 1315–1325.

R Core Team (2013). R: A language and environment for statistical computing (Vienna, Austria: R Foundation for Statistical Computing), http://www.R-project.org/.

Rahman, M.T., Ghosh, C., Hossain, M., Linfield, D., Rezaee, F., Janigro, D., Marchi, N., and van Boxel-Dezaire, A.H.H. (2018). IFN-γ, IL-17A, or zonulin rapidly increase the permeability of the blood-brain and small intestinal epithelial barriers: relevance for neuro-inflammatory diseases. Biochem. Biophys. Res. Commun. 507, 274–279.

Rea, K., Dinan, T.G., and Cryan, J.F. (2016). The microbiome: a key regulator of stress and neuroinflammation. Neurobiol. Stress 4, 23–33.

Reger, M.A., Henderson, S.T., Hale, C., Cholerton, B., Baker, L.D., Watson, G.S., Hyde, K., Chapman, D., and Craft, S. (2004). Effects of beta-hydroxybutyrate on cognition in memory-impaired adults. Neurobiol. Aging 25, 311–314.

Reikvam, D.H., Erofeev, A., Sandvik, A., Grcic, V., Jahnsen, F.L., Gaustad, P., McCoy, K.D., Macpherson, A.J., Meza-Zepeda, L.A., and Johansen, F.E. (2011). Depletion of murine intestinal microbiota: effects on gut mucosa and epithelial gene expression. PLoS One 6, e17996.

Ruskin, D.N., Fortin, J.A., Bisnauth, S.N., and Masino, S.A. (2017). Ketogenic diets improve behaviors associated with autism spectrum disorder in a sex-specific manner in the EL mouse. Physiol. Behav. 168, 138–145.

Cell Host & Microbe
Article

CellPress

Samala, R., Willis, S., and Borges, K. (2008). Anticonvulsant profile of a balanced ketogenic diet in acute mouse seizure models. Epilepsy Res *81*, 119–127.

Sampson, T.R., and Mazmanian, S.K. (2015). Control of brain development, function, and behavior by the microbiome. Cell Host Microbe *17*, 565–576.

Savignac, H.M., Tramullas, M., Kiely, B., Dinan, T.G., and Cryan, J.F. (2015). Bifidobacteria modulate cognitive processes in an anxious mouse strain. Behav. Brain Res. *287*, 59–72.

Sbihi, H., Boutin, R.C., Cutler, C., Suen, M., Finlay, B.B., and Turvey, S.E. (2019). Thinking bigger: how early-life environmental exposures shape the gut microbiome and influence the development of asthma and allergic disease. Allergy *74*, 2103–2115.

Schneider, C.A., Rasband, W.S., and Eliceiri, K.W. (2012). NIH Image to ImageJ: 25 years of image analysis. Nat. Methods *9*, 671–675.

Shen, Y., Zhang, Y., Chen, L., Du, J., Bao, H., Xing, Y., Cai, M., and Si, Y. (2020). Chemokine CXCL13 acts via CXCR5-ERK signaling in hippocampus to induce perioperative neurocognitive disorders in surgically treated mice. Journal of neuroinflammation *17*, 335.

Shenghua, P., Ziqin, Z., Shuyu, T., Huixia, Z., Xianglu, R., and Jiao, G. (2020). An integrated fecal microbiome and metabolome in the aged mice reveal anti-aging effects from the intestines and biochemical mechanism of FuFang zhen-shu TiaoZhi(FTZ). Biomed. Pharmacother. *121*, 109421.

Solis, E., Hascup, K.N., and Hascup, E.R. (2020). Alzheimer's disease: the link Between amyloid-β and neurovascular dysfunction. J. Alzheimers Dis. *76*, 1179–1198.

Summanen, P.H., Jousimies-Somer, H., Manley, S., Bruckner, D., Marina, M., Goldstein, E.J., and Finegold, S.M. (1995). Bilophila wadsworthia isolates from clinical specimens. Clin. Infect. Dis. *20* (suppl 2), S210–S211.

Sweeney, M.D., Sagare, A.P., and Zlokovic, B.V. (2018). Blood-brain barrier breakdown in Alzheimer disease and other neurodegenerative disorders. Nat. Rev. Neurol. *14*, 133–150.

Swerdlow, N.R., and Geyer, M.A. (1998). Using an animal model of deficient sensorimotor gating to study the pathophysiology and new treatments of schizophrenia. Schizophr. Bull. *24*, 285–301.

Szklarczyk, D., Gable, A.L., Lyon, D., Junge, A., Wyder, S., Huerta-Cepas, J., Simonovic, M., Doncheva, N.T., Morris, J.H., Bork, P., et al. (2019). STRING v11: protein-protein association networks with increased coverage, supporting functional discovery in genome-wide experimental datasets. Nucleic Acids Res *47*, D607–D613.

Ta, T.T., Dikmen, H.O., Schilling, S., Chausse, B., Lewen, A., Hollnagel, J.O., and Kann, O. (2019). Priming of microglia with IFN-γ slows neuronal gamma oscillations in situ. Proc. Natl. Acad. Sci. USA *116*, 4637–4642.

Takahara, M., Takaki, A., Hiraoka, S., Adachi, T., Shimomura, Y., Matsushita, H., Nguyen, T.T.T., Koike, K., Ikeda, A., Takashima, S., et al. (2019). Berberine improved experimental chronic colitis by regulating interferon-γ- and IL-17A-producing lamina propria CD4+ T cells through AMPK activation. Sci. Rep. *9*, 11934.

Takeuchi, H., Wang, J., Kawanokuchi, J., Mitsuma, N., Mizuno, T., and Suzumura, A. (2006). Interferon-gamma induces microglial-activation-induced cell death: a hypothetical mechanism of relapse and remission in multiple sclerosis. Neurobiol. Dis. *22*, 33–39.

Titus, A.D., Shankaranarayana Rao, B.S., Harsha, H.N., Ramkumar, K., Srikumar, B.N., Singh, S.B., Chattarji, S., and Raju, T.R. (2007). Hypobaric hypoxia-induced dendritic atrophy of hippocampal neurons is associated with cognitive impairment in adult rats. Neuroscience *145*, 265–278.

Tripathi, A., Melnik, A.V., Xue, J., Poulsen, O., Meehan, M.J., Humphrey, G., Jiang, L., Ackermann, G., McDonald, D., Zhou, D., et al. (2018). Intermittent hypoxia and hypercapnia, a hallmark of obstructive sleep apnea, alters the gut microbiome and metabolome. mSystems *3*, e00020–18.

Valentini, F., Evangelisti, M., Arpinelli, M., Di Nardo, G., Borro, M., Simmaco, M., and Villa, M.P. (2020). Gut microbiota composition in children with obstructive sleep apnoea syndrome: a pilot study. Sleep Med *76*, 140–147.

van Berkel, A.A., IJff, D.M., and Verkuyl, J.M. (2018). Cognitive benefits of the ketogenic diet in patients with epilepsy: A systematic overview. Epilepsy Behav *87*, 69–77.

van de Wouw, M., Boehme, M., Lyte, J.M., Wiley, N., Strain, C., O'Sullivan, O., Clarke, G., Stanton, C., Dinan, T.G., and Cryan, J.F. (2018). Short-chain fatty acids: microbial metabolites that alleviate stress-induced brain-gut axis alterations. J. Physiol. *596*, 4923–4944.

Vinciguerra, F., Graziano, M., Hagnäs, M., Frittitta, L., and Tumminia, A. (2020). Influence of the Mediterranean and ketogenic diets on cognitive status and decline: a narrative review. Nutrients *12*, 1019.

Vogt, N.M., Kerby, R.L., Dill-McFarland, K.A., Harding, S.J., Merluzzi, A.P., Johnson, S.C., Carlsson, C.M., Asthana, S., Zetterberg, H., Blennow, K., et al. (2017). Gut microbiome alterations in Alzheimer's disease. Sci. Rep. *7*, 13537.

von Bohlen und Halbach, O. (2011). Immunohistological markers for proliferative events, gliogenesis, and neurogenesis within the adult hippocampus. Cell Tissue Res *345*, 1–19.

Vuong, H.E., and Hsiao, E.Y. (2017). Emerging roles for the gut microbiome in autism spectrum disorder. Biol. Psychiatry *81*, 411–423.

Vuong, H.E., Yano, J.M., Fung, T.C., and Hsiao, E.Y. (2017). The microbiome and host behavior. Annu. Rev. Neurosci. *40*, 21–49.

Wei, L., Yao, M., Zhao, Z., Jiang, H., and Ge, S. (2018). High-fat diet aggravates postoperative cognitive dysfunction in aged mice. BMC Anesthesiol *18*, 20.

Yu, F., Han, W., Zhan, G., Li, S., Xiang, S., Zhu, B., Jiang, X., Yang, L., Luo, A., Hua, F., and Yang, C. (2019). Abnormal gut microbiota composition contributes to cognitive dysfunction in streptozotocin-induced diabetic mice. Aging (Albany, NY) *11*, 3262–3279.

Zhang, J., He, H., Qiao, Y., Zhou, T., He, H., Yi, S., Zhang, L., Mo, L., Li, Y., Jiang, W., and You, Z. (2020). Priming of microglia with IFN-γ impairs adult hippocampal neurogenesis and leads to depression-like behaviors and cognitive defects. Glia *68*, 2674–2692.

Zhao, Q., Stafstrom, C.E., Fu, D.D., Hu, Y., and Holmes, G.L. (2004). Detrimental effects of the ketogenic diet on cognitive function in rats. Pediatr. Res. *55*, 498–506.

Zhao, Y., and Gong, C.X. (2015). From chronic cerebral hypoperfusion to Alzheimer-like brain pathology and neurodegeneration. Cell. Mol. Neurobiol. *35*, 101–110.

Zhou, X., Zöller, T., Krieglstein, K., and Spittau, B. (2015). TGFβ1 inhibits IFNγ-mediated microglia activation and protects mDA neurons from IFNγ-driven neurotoxicity. J. Neurochem. *134*, 125–134.

Zhu, X., Lee, H.G., Perry, G., and Smith, M.A. (2007). Alzheimer disease, the two-hit hypothesis: an update. Biochim. biophys. acta *1772*, 494–502.

Ziehn, M.O., Avedisian, A.A., Dervin, S.M., O'Dell, T.J., and Voskuhl, R.R. (2012). Estriol preserves synaptic transmission in the hippocampus during autoimmune demyelinating disease. Lab. Invest. *92*, 1234–1245.

STAR★METHODS

KEY RESOURCES TABLE

REAGENT or RESOURCE	SOURCE	IDENTIFIER
Antibodies		
anti-DCX (Guinea Pig Polyclonal)	Millipore	Cat#AB2253
IL-17A Monoclonal Antibody (eBio17B7), FITC	ThermoFisher	Cat#11-7177-81
IFN gamma Monoclonal Antibody, (XMG1.2), PE	ThermoFisher	Cat#12-7311-81
CD3 Monoclonal Antibody, (17A2), APC	BioLegend	Cat#100236
CD4 Monoclonal Antibody, (GK1.5), PE-eFluor 610	ThermoFisher	Cat#61-0041-80
CD45 Monoclonal Antibody, (30-F11), BV605	BioLegend	Cat#103140
Bacterial and virus strains		
Clostridium cocleatum	Deutsche Sammlung von Mikroorganismen und Zellkulturen (DSMZ)	DSMZ# 1551
Bilophila wadsworthia	Murine-associated strain gifted from Drs. Connie Ha and Suzanne Devkota	Strain WAL7959
Chemicals, peptides, and recombinant proteins		
Vancomycin hydrochloride	Chem-Impex International	Cat#00315
Neomycin trisulfate salt hydrate	Sigma-Aldrich	Cat#N1876
Metronidazole	Sigma-Aldrich	Cat#M1547
Ampicillin sodium salt	Sigma-Aldrich	Cat#A9518
NaCl	Sigma-Aldrich	Cat#S7653
KCl	Sigma-Aldrich	Cat#P3911
$NaHCO_3$	Sigma-Aldrich	Cat#S5761
NaH_2PO_4	Sigma-Aldrich	Cat#S0751
$CaCl_2$	Sigma-Aldrich	Cat#C1016
$MgSO_4$	Sigma-Aldrich	Cat#M7506
Glucose	Sigma-Aldrich	Cat#47829
Brucella media	Hardy Diagnostics	Cat#C5311
Ferric ammonium citrate	Fisher Scientific	Cat#172-500
DAKO antigen retrieval solution	Agilent	Cat#S1699
RPMI 1640	Sigma-Aldrich	Cat#11875093
EDTA	ThermoFisher	Cat#15575020
HEPES	ThermoFisher	Cat#15630080
HBSS	ThermoFisher	Cat#14170112
Collagenase D	Sigma Aldrich	Cat#11088866001
DNAse I, Grade II	Sigma Aldrich	Cat#10104159001
Dispase	Gibco	Cat#17105041
Ionomycin calcium salt	Sigma Aldrich	Cat#I3909
PMA	Sigma Aldrich	Cat#P1585
Brefeldin A	Sigma Aldrich	Cat#B7651
MEM NEAA	ThermoFisher	Cat#10370021
Penicillin-streptomycin (Pen/strep)	ThermoFisher	Cat#15070063
Ultrapure water	ThermoFisher	Cat#10977015
DNA intercalating dye (EvaGreen)	Biotium	Cat#31000
Sodium pyruvate	Gibco	Cat#11360070

(Continued on next page)

Cell Host & Microbe
Article

CellPress

Continued		
REAGENT or RESOURCE	SOURCE	IDENTIFIER
Critical commercial assays		
DNeasy PowerSoil Kit	Qiagen	Cat#12888-50
Qiaquick PCR purification kit	Qiagen	Cat#28104
RNEasy Mini Kit	Qiagen	Cat#74104
QuantSeq FWD' mRNA-Seq Library Prep Kit	Lexogen	N/A
LIVE/DEAD™ Fixable Aqua Dead Cell Stain Kit	ThermoFisher	Cat#L34957
Intracellular Fixation & Permeabilization Buffer Set	ThermoFisher	Cat#88-8824-00
QX200 ddPCR EvaGreen Supermix	Bio-Rad Laboratories	Cat#186-4033
V-PLEX Proinflammatory Panel 1 Mouse Kit	Meso Scale Diagnostics	Cat#K15048D
Deposited data		
16S rRNA gene sequencing		Study ID: 13510
Hippocampal transcriptomic data	Gene Expression Omnibus	Study ID: GSE163099
Experimental models: Organisms/strains		
Swiss Webster mice	Taconic Farms	Cat#Tac:SW
C57BL6/J mice	Jackson Laboratories	Cat#000664
T-bet TBX21 knockout mice (B6.129S6-*Tbx21tm1Glm*/J)	Jackson Laboratories	Cat#004648
Oligonucleotides		
Forward primer for digital PCR: UN00F2, 5'- CAGCMGCCGCGGTAA-3	Integrated DNA Technologies	N/A
Reverse primer for digital PCR: UN00R0, 5'-GGACTACHVGGGTWTCTAAT-3' [1, 3])	Integrated DNA Technologies	N/A
Software and algorithms		
EthoVision XT	Noldus	
Deblur	https://github.com/biocore/deblur	Amir et al., 2017
QIIME2-2018.6	https://qiime2.org/	Bolyen et al.
FastQC v. 0.11.9	https://github.com/s-andrews/FastQC/releases/tag/v0.11.9	Andrews, 2010
Trimmomatic	https://github.com/timflutre/trimmomatic	Bolger et al.
HISAT2	http://daehwankimlab.github.io/hisat2/	Kim et al.
HTSeq-count	https://github.com/htseq/htseq	Anders et al.
DESeq2	https://bioconductor.org/packages/release/bioc/html/DESeq2.html	Love et al.
R package	https://www.r-project.org/	R Core Team, 2013
DAVID	https://david.ncifcrf.gov/gene2gene.jsp	Huang da et al., 2009a, 2009b
STRING	https://string-db.org/	Szklarczyk et al., 2019
QuantaSoft Software	Bio-Rad Laboratories	Cat#1864011
Prism software version 8.2.1	GraphPad	
Other		
"Breeder" chow	Lab Diets	Cat#5K52
Standard chow	Lab Diets	Cat#5010
Ketogenic diet	Harlan Teklad	Cat#TD.1150300
Control diet	Harlan Teklad	Cat#TD.150300
O2 Control InVivo cabinet	Coy Laboratories	Cat#Model 30
GigE camera	Basler	Cat#acA1280-60gc
4200 Tapestation System	Agilent	Cat#G2991AA
QX200 Droplet Generator	Bio-Rad Laboratories	Cat#1864002

RESOURCE AVAILABILITY

Lead contact
Further information and requests for resources and reagents should be directed to and will be fulfilled by the Lead Contact, Elaine Hsiao (ehsiao@g.ucla.edu)

Materials availability
This study did not generate new unique reagents.

Data and code availability
16S rRNA gene sequencing data and metadata are available through QIITA repository (https://qiita.ucsd.edu/) with the study accession # 13510. Hippocampal transcriptomic data are available on through Gene Expression Omnibus repository (https://www.ncbi.nlm.nih.gov/geo/) with the identification number # GSE163099.

EXPERIMENTAL MODELS AND SUBJECT DETAILS

Mice
4–6-week-old SPF wild-type Swiss Webster mice (Taconic Farms), GF wild-type Swiss Webster mice (Taconic Farms), SPF wild-type C57BL6/J mice (Jackson Laboratories), GF wild-type C57BL6/J (Jackson Laboratories), and SPF T-bet TBX21 knockout mice (B6.129S6-*Tbx21tm1Glm*/J, Jackson Laboratories) were bred in UCLA's Center for Health Sciences Barrier Facility. Mice were randomly assigned to an experimental group. Experiments include age- and sex-matched cohorts of males and females. Mice were housed in autoclaved cages with irradiated food and sterile water and handled aseptically in a BSL2 biosafety cabinets with autoclaved gloves and sterile consumables. All animal experiments were approved by the UCLA Animal Care and Use Committee.

Bacteria
Bilophila wadsworthia (strain WAL7959), generously provided by Drs. Connie Ha and Suzanne Devkota (Cedars-Sinai Medical Center, Los Angeles, CA), was cultured under anoxic conditions (2–3% H_2, 20% CO_2, and the balance N_2) at 37°C in Modified Brucella media supplemented with 1% taurine, iron, hemin, and vitamin K (Hardy Diagnostics). *Clostridium cocleatum* (DSMZ 1551) was grown under anoxic conditions (2–3% H_2, 20% CO_2, and the balance N_2) at 37°C in sweet e. broth for anaerobes (ATCC medium 1004). Cultures were authenticated by full-length 16S rRNA gene sequencing (Laragen, Inc.).

METHOD DETAILS

Dietary treatment
Breeding GF mice were fed sterile "breeder" chow (Lab Diets 5K52). Experimental animals were either fed sterile standard chow (Lab Diets 5010), 6:1 ketogenic diet (Harlan Teklad TD.1150300), or vitamin- and mineral-matched control diet (Harlan Teklad TD.150300).

Acute intermittent hypoxia
Mice housed in the home cage were placed in an O2 Control *invivo* cabinet (Coy Laboratories) and exposed to 12% oxygen for 6 h per day for 5 consecutive days. Mock-treated mice were placed in the same chamber and exposed to ambient 21% oxygen for 6 h per day for 5 consecutive days.

Barnes maze testing
Mice were tested for cognitive behavior in the Barnes maze (92 cm diameter, 5 cm hole diameter, 95 cm height; Noldus) using aseptic technique and procedures adapted from a previously published protocol (Attar et al., 2013). For GF mice, the absence of colonization was confirmed at the end of Barnes maze testing by fecal microbial culture under aerobic and anaerobic conditions, 16S rRNA gene qPCR relative to untested GF controls, and visual confirmation of enlarged cecal size consistent with GF status. Briefly, mice were acclimated for at least 1 hour before testing to the behavioral room, which featured consistent visual cues that varied in shape, color, and placement. The maze was cleaned before and after each testing trial with 70% ethanol, followed by Accel disinfectant. All sessions were recorded using a Basler Gig3 camera and EthoVision XT (Noldus). For the habituation phase (day 1), mice were placed in a clear glass beaker in the center of the maze for 30 seconds, then slowly guided to the target hole and gently pushed into the escape box if they did not enter on their own accord. Mice were kept in the escape box for 1 min and then allowed to explore the maze freely for 5 min before being returned to their home cages. During the training phase (Day 2-3), mice were tested for 3 trials on the first day, and 2 trials for the second day. For each trial, mice were first placed under an opaque cup in the center of the maze for 15 seconds. Then, the cylinder was removed, and mice were allowed to explore the maze for 5 min. Latency to enter was defined as the time elapsed for mice to identify the target hole correctly for the first time. Errors made were defined as nose pokes over incorrect holes. Distance traveled, velocity, and time in each quadrant were other recorded for every trial. Search strategy was also analyzed, where a "random" strategy was coded as greater than 3 errors in non-consecutive holes, a "serial" strategy was coded as errors occurring in consecutive holes, and a "spatial" strategy was coded as less than or equal to 3 hole errors. The probe trial (Day 4) was performed

Cell Host & Microbe
Article

CellPress

24 h after the final training trial. The escape box was removed, and mice were allowed to explore the maze for 5 min while latency to enter, distance traveled, errors made, velocity, search strategy and time in target were recorded.

Open field testing

The open field test is widely used to measure anxiety-like and locomotor behavior in rodents. Mice were placed in the center of a 50 cm x 50 cm arena for 10 min, during which an overhead Basler Gig3 camera and EthoVision XT (Noldus) software was used to measure distance traveled, and the number of entries and duration of time spent in the central 17 cm square area. The boxes were cleaned with 70% ethanol and Accel disinfectant before and after each session.

Prepulse inhibition testing

Prepulse inhibition is used to measure sensorimotor gating and acoustic startle and was performed according to protocols adapted from (Hsiao, 2013; Swerdlow and Geyer, 1998) in the UCLA Behavioral Testing Core (Franz Hall). Mice were acclimated to an SR-LAB testing chamber (SD Instruments) for 5 min, presented with six 120-dB pulses of white noise (startle stimulus), and then subjected to 14 randomized blocks of either no startle, 5-dB prepulse + startle, or 15-dB prepulse + startle. The startle response was recorded by a piezo-electric sensor and prepulse inhibition was defined as (startle stimulus only -5 or 15 dB prepulse + startle)/ startle stimulus only x 100.

Antibiotic treatment

SPF mice were gavaged every 12 h daily for 7 consecutive days with a solution of vancomycin (50mg/kg), neomycin (100 mg/kg) and metronidazole (100 mg/kg), as previously described (Reikvam et al., 2011). Ampicillin (1 mg/ml) was provided *ad libitum* in sterile drinking water. For mock treatment, mice were gavaged with normal drinking water every 12 h daily for 7 days. Antibiotic-treated mice were maintained in sterile caging with sterile food and water and handled aseptically for the remainder of the experiments.

Fecal microbiota transplant

Fresh fecal samples were obtained from adult SPF Swiss Webster homogenized in 1 mL pre-reduced phosphate-buffered saline (PBS, pH = 7.4) per pellet. 100 μL of the suspension was immediately administered via oral gavage to recipient GF mice. For mock treatment, mice were gavaged with pre-reduced PBS.

16S rRNA gene sequencing

Total bacterial genomic DNA was extracted from mouse fecal samples using the Qiagen DNeasy PowerSoil Kit, where sample n reflects separate cages containing 2 mice per cage to reduce cage-dependent effects of variation and focus on biological variation. The library was prepared following previously published and validated methods (Caporaso et al., 2011). The V4 regions of the 16S rDNA gene were PCR amplified using individually barcoded universal primers and 30 ng of the extracted genomic DNA. The PCR reaction was set up in triplicate, and the PCR products were purified using the Qiaquick PCR purification kit (Qiagen). The purified PCR product was pooled in equal molar concentrations quantified by nanodrop and sequenced by Laragen, Inc. using the Illumina MiSeq platform and 2 x 250bp reagent kit for paired-end sequencing. Amplicon sequence variants (ASVs) were chosen after denoising with Deblur (Amir et al., 2017). Taxonomy assignment and rarefaction were performed using QIIME2-2018.6 (Bolyen et al., 2019)

Gnotobiotic colonization and antibiotic enrichment

10^9 cfu bacteria were suspended in 200 μL pre-reduced PBS and orally gavaged into GF mice or Abx-treated mice. For mock treatment, mice were gavaged with pre-reduced PBS. Mice were maintained in microisolator cages and handled aseptically. Mice were behaviorally tested 7 days post-colonization. Colonization was confirmed via fecal plating on modified Brucella agar supplemented with 0.5 g/L ferric ammonium citrate.

Hippocampal electrophysiology

For long-term potentiation, paired-pulse-facilitation, and population spike versus fEPSP slopes, we used protocols as previously described (Babiec et al., 2017; Ziehn et al., 2012). Based on prior literature the detrimental effects of Hyp on cognitive behavior primarily in male mice (Aubrecht et al., 2015, males were used for hippocampal electrophysiology. Mice were first deeply anesthetized with isoflurane, and following cervical dislocation, the brain was rapidly removed and submerged in ice-cold, oxygenated (95% O2/5% CO2) artificial cerebrospinal fluid (ACSF) containing (in mM) as follows: 124 NaCl, 4 KCl, 25 $NaHCO_3$, 1 NaH_2PO_4, 2 $CaCl_2$, 1.2 $MgSO_4$, and 10 glucose (Sigma-Aldrich). While iced, the brain was hemisected, and the hippocampi removed. Slice were made using a manual tissue chopper in 400 μM sections and maintained at 30°C in interface-type chambers that were continuously perfused (2–3 ml/min) with oxygenated (95% O2/5% CO2) ACSF and allowed to recover in the interface chambers for at least 2 h before recordings. For all experiments, a bipolar nichrome wire stimulating electrode was placed in stratum radiatum of the CA1 region and used to activate Schaffer collateral fiber synapses. For paired pulse facilitation and population spike measurements, the recording electrode was placed in the pyramidal cell body layer. All recordings (LTP, paired pulse facilitation, and population spike measurements) were performed using borosilicate glass microelectrodes (5-10 M Ω) filled with ACSF and using an Ag/AgCl electrode. The stimulating and recording electrodes were placed approximately 0.75-1.0 mm apart for each assay. For LTP recordings, the initial maximal fEPSP amplitude was determined and the intensity of stimulation was adjusted to produce fEPSPs with an

amplitude 50% of the maximal amplitude for all recorded responses to stimulus. Baseline recordings were taken for at least 20 min, followed by two trains of 1 second long 100 Hz stimulation with 10 seconds inter-train interval, then 60 min recording post-tetanus. The last 5 min of the 60 min recording post-tetanus were used for statistical comparison. Paired-pulse facilitation was measured at impulse distances of 10, 20, 30, 40 and 50 ms by measuring the height of the population spike. Acquisition and analysis of data was performed with the pClamp family of programs from Axon Instruments Inc (Burlingame, CA). Slices were included if they showed a stable baseline, with fEPSP slides within 5% error of each other, for 20 minutes. Separate slices were used for recording LTP vs. paired pulse facilitation.

Hippocampal transcriptomic profiling

Hippocampi were microdissected and RNA extracted using the Qiagen RNEasy Mini Kit. RNA quality was assessed to be RIN>8.9 using the 4200 Tapestation (Agilent). RNA libraries were prepared using the QuantSeq FWD' mRNA-Seq Library Prep Kit (Lexogen) and sequenced via the Illumina HiSeq platform by the UCLA Neuroscience Genomics Core. Sequences were filtered using FastQC v. 0.11.9 (Andrews, 2010) for quality control, followed by Trimmomatic (Bolger et al., 2014) to remove barcodes and reads with an average phred score of 33 (parameters: illuminaclip:2:30:6, slidingwindow:5:30, leading:30, trailing:30, crop:65, minlen:20). Parsed reads were then aligned to the mouse genome mm10 using HISAT2 (Kim et al., 2019). Read counts were obtained using HTSeq-count (Anders et al., 2015). Differential gene expression was determined using DESeq2 (Love et al., 2014). Heatmaps were constructed using the R package (Team, 2013) pheatmap (Kolde, 2015), GO term enrichment analysis was conducted using DAVID (Huang da et al., 2009a, 2009b) and Protein-Protein network analysis using STRING (Szklarczyk et al., 2019).

Hippocampal immunofluorescence staining and imaging

Hippocampi were microdissected, post-fixed in 4% paraformaldehyde for 24 h, cryopreserved in 30% sucrose for 24 h, embedded and frozen in OCT, and cryosectioned using a Leica CM1950 cryostat. 25 μm coronal sections were collected within a span of 200 μm and distributed between two slides beginning at the site of the hippocampal formation, determined in accordance to the Mouse P56 Coronal Reference Atlas of the Allen Institute (Lein et al., 2007). Slides were incubated in DAKO antigen retrieval solution (Agilent) at 90 °C for 2 min, washed, and then blocked (0.3%PBS-T, 5% BSA, 10% normal goat serum) for 1 h at room temperature. Sections were incubated at 4°C for 48 h using anti-DCX (Guinea Pig Polyclonal, 1:500, Millipore AB2253), washed and then incubated with Alexa Fluor secondaries (1:1000) for 2 h at room temperature before being washed and mounted. Sections were imaged using a Zeiss LSM 780 confocal microscope at 20X magnification with 1.5 zoom across 8.4 μm section widths across 7 Z-stacks. Image optimization and orthogonal projections were performed in Zen Blue (Zeiss) and background removal was done in ImageJ (Schneider et al., 2012). Quantification of DCX was performed by tracing the granule cell layers of the DG and quantitating DCX+ within enclosed area using ImageJ (NIH) particle analysis (Schneider et al., 2012).

Lymphocyte isolation and flow cytometry

Single-cell suspensions were prepared from colonic lamina propria using procedures adapted from (Takahara et al., 2019). Colons were dissected, cut longitudinally with gentle fat removal, and contents washed away in 1 X PBS. Epithelial cell stripping was achieved through two 45-minute incubations shaking at 37 °C HBSS with 0.5M EDTA and 1M HEPES (ThermoFisher). Colonic tissue was then digested using two 45-minute incubations shaking at 37 °C in RPMI supplemented with 4% FCS, 0.5 mg/mL collagenase D (Sigma), 0.25 mg/mL DNAseI, grade II (Sigma), and 0.5 mg/mL dispase (Gibco). All lymphocytes were then collected and stimulated for 2 h with 500 ng/mL PMA and 500 ng/mL ionomycin in RPMI with 10% FCS, 2% MEM NEAA, 2% Pen/strep, 2% sodium pyruvate, followed by 3-hour incubation with 500 ng/mL Brefeldin A. Cells were incubated on ice and in darkness with 1:600 viability dye for 20 min, followed by 30 min incubation on ice and in darkness with CD3-APC (Biolegend), CD4-PE (ThermoFisher), CD45-BV605 (Biolegend) at 1:200 in FACS buffer. Cells were next incubated with 100 μL of fixation buffer for 30 min in darkness, washed with 1X PBS, and stored in PBS at 4 °C until the next day. On the following day, cells were incubated with permeabilization buffer for 15 min in darkness at room temperature, followed by intracellular antibodies IL-17A- FITC (ThermoFisher) and IFNg-PE (ThermoFisher) for 30 min on ice in darkness at a 1:200 ratio in permeabilization buffer. Data were acquired on FACSCalibur (BD Biosciences) or the Attune NxT Flow Cytometer. All data contained within a graph were acquired on the same flow cytometer (GF data on the FACSCalibur, and Abx and SPF data on the Attune NxT, respectively). Data were analyzed using FlowJo (TreeStar) software.

Digital PCR

Briefly, each reaction was set up with 92.0 μL of DNA sample, 10 μL of ddPCR master mix (QX200 ddPCR EvaGreen Supermix, Bio-Rad Laboratories), forward (UN00F2, 5′- CGCCGGTATCGAAATCGTGACAGCMGCCGCGGTAA-3′) and reverse (UN00R0, 5′-ATTCGCGGAAGGAGCGAGAG GGACTACHVGGGTWTCTAAT-3′ [1, 3]) primers (Integrated DNA Technologies) at the final concentration of 500 nM each, and ultrapure water (Thermo Fisher Scientific) to the final volume of 20 μL. In some experiments, additional DNA intercalating dye (EvaGreen, Biotium) was added to the reactions up to ×1 final concentration (to achieve up to ×2 overall concentration). Each reaction volume was converted to droplets using a QX200 droplet generator (Bio-Rad Laboratories). Droplet samples were amplified on a thermocycler (C1000 Touch, Bio-Rad Laboratories) with the following conditions according to the program: initial denaturation at 95°C for 5 min. followed by 40 cycles each consisting of denaturation at 95°C for 30 sec., annealing at 6552°C for 30 sec., and extension at 68°C for 60 sec.; followed by the dye stabilization step consisting of 5 min incubation at 4°C, 5 min incubation at 90°C, and incubation at 12°C for at least 5 min. Droplet samples were quantified on a QX200 Droplet Digital PCR System

Cell Host & Microbe
Article

CellPress

(Bio-Rad Laboratories). The raw data were analyzed and the target molecule Sample concentrations were extracted using the accompanying software (QuantaSoft Software, Bio-Rad Laboratories) with auto-thresholding conditions. Sample concentrations were then normalized to sample extraction mass and corrected for volume losses during extraction protocol. Lower limit of quantification of the assay was determined as 3X the no template control concentration normalized to the minimum sample extraction mass.

Serum cytokine quantification

Blood samples were collected by cardiac puncture and spun through serum separation tubes (SST vacutainers, Becton Dickinson). Serum IFNg, IL-2, IL-4, IL-1β, TNFα, KC/GRO, IL-4, IL-5, and IL-10 concentrations were quantified using the V-PLEX Proinflammatory Panel 1 Mouse Kit (Meso Scale Diagnostics), according to the manufacturer's instructions.

QUANTIFICATION AND STATISTICAL ANALYSIS

Statistical analysis was performed using Prism software version 8.2.1 (GraphPad). Data were assessed for normal distribution and plotted in the figures as mean ± SEM. For each figure, n = the number of independent biological replicates. No samples or animals were excluded from the analyses. Differences between two treatment groups were assessed using two-tailed, unpaired Student's t test with Welch's correction. Differences among >2 groups with only one variable were assessed using one-way ANOVA with Sidak post hoc test. Taxonomic comparisons from 16S rDNA gene sequencing analysis were analyzed by Kruskal-Wallis test with Bonferroni *post hoc* test. Two-way ANOVA with Sidak *post-hoc* test was used for $\geq$ 2 groups with two variables (e.g., Barnes maze latency to enter, errors made over 6 trials). Significant differences emerging from the above tests are indicated in the figures by $^*p < 0.05$, $^{**}p < 0.01$, $^{***}p < 0.001$, $^{****}p < 0.0001$. Notable non-significant (and non-near significant) differences are indicated in the figures by "n.s."